Distribution: Restricted

Delivery report

TerrA-P: Development and validation of a global GPP/NPP model using MERIS and Sentinel-3 data

Validation report

Manuela Balzarolo, Ivan Janssens, Sara Vicca, Iain Colin Prentice, Rebecca Thomas, Else Swinnen, Roel Van Hoolst

Study accomplished under the authority of ESA

February 2018

DISTRIBUTION LIST

Philippe Goryl, ESA-ESRIN

Else Swinnen, VITO
Roel Van Hoolst, VITO
Bruno Smets, VITO

Iain Colin Prentice, ICL
Rebecca Thomas, ICL

Ivan Janssens, UA
Manuela Balzarolo, UA*
Sara Vicca, UA

*now working at CREAF, Global Ecology Unit CREAF-CSIC-UAB, Spain

TABLE OF CONTENTS

LIST OF FIGURES

LIST OF TABLES

LIST OF ACRONYMS

CRO	Cropland
DBF	Deciduous Broadleaf Forest
EBF	Evergreen Broadleaf Forest
ECMWF	European Centre for Mid-range Weather Forecast
EO	Earth Observation
ENF	Evergreen Needleleaf Forest
FAPAR	Fraction of absorbed photosynthetically active radiation
GPP	Gross Primary Productivity
GRA	Grassland
ICL	Imperial College London
LUE	Light use efficency
LST	Land surface temperature
MAE	Mean absolute error
MERIS	Medium Resolution Imaging Spectrometer
MF	Mixed forest
OSH	Open Scrublands
pBias	Percentage bias
PFT	Plant functional type
Rg	Incoming shortwave global radiation
RMSE	Root mean squared error
R^2	Coefficient of determination
SAV	Savanna
Ta	Air temperature
UA	Universiteit Antwerpen
VITO	Vlaamse Instelling voor Technologisch Onderzoek
WSA	Woody Savanna

CHAPTER 1 DEFINITION

1.1. SCOPE AND OBJECTIVES

The purpose of this document is to report the results of the model validation at global scale against in-situ observations of GPP. It focuses on the validation of model simulations based on MERIS fAPAR input data.

1.2. APPLICABLE DOCUMENTS

[AD1] Algorithm Theoretical Basis Document v2

1.3. CONTENT OF THE DOCUMENT

The validation report is organized in the following way:

- **Chapter 2** details on the validation approach using in-situ data.
- **Chapter 3** results of the model performance at global scale.

CHAPTER 2 GPP DATA DESCRIPTION

The GPP data were derived using the model described in V2 of the ATBD [AD1].
The performance of following model simulations are validated:

1) **ECMWF**: model driven by ECMWF air temperature and mean dekad minimum and maximum was used to calculate the vapor pressure deficit (VPD).
2) **LST**: model driven by land surface temperature (LST) and mean dekad temperature was used to calculate VPD.

The details of the input data to generate these two sets of GPP estimates are provided in *Table 1*.

Parameter	Source	Input data	
		ECMWF	LST
Daily incoming radiation [kJ/m2/d]	ECMWF, 10-daily averages at 0.25° grid	X	X
Daily mean temperature [°C]	ECMWF, 10-daily averages at 0.25° grid	X	
Daily min temperature [°C]	ECMWF, 10-daily averages at 0.25° grid	X	
Daily max temperature [°C]	ECMWF, 10-daily averages at 0.25° grid	X	
Average water vapour pressure [hPa]	ECMWF, 10-daily averages at 0.25° grid	X	X
fAPAR [-]	MERIS GVI, 1 km, 10-daily	X	X
LST [°C]	AATSR level 2, 1 km, cloud-free daytime observations, gap-filled and Swets smoothed		X

Table 1: Input data for GPP estimation.

CHAPTER 3 VALIDATION APPROACH

This chapter describes the validation approach of the model simulations. The point location model simulations are validated with in-situ data of Gross Primary Productivity (GPP).

3.1. VALIDATION AGAINST IN-SITU DATA

This validation aims to evaluate the performance of models in simutating inter-annual, spatial and seasonal variability of GPP for a variety of ecosystems. More specifically we tested how well the model simulations: (i) encompass the seasonal trends of GPP; (ii) describe annual carbon dynamics for different ecosystems (e.g. forests, grasslands, croplands, wetlands, tundra); (iii) describe interannual variability; (iv) describe the GPP-Rg ecological function.

The validation was performed only for the years for which the remote sensed product matches the in-situ observations. In particular, the analysis is based on 58 sites for ECMWF model simulations while 46 sites for LST simulations. A different number of sites for each model validation have been selected for an indipent validation of the two models. For model benmarcking only we used the same number of the sites. More details on “Site selection” and data quality are reported in the section 3.1.1.

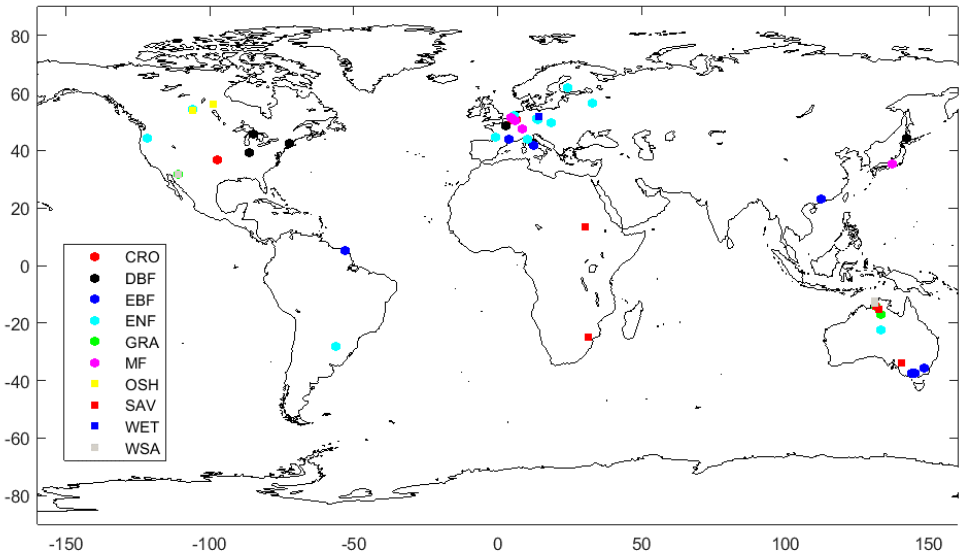

Figure 1 shows the geographical distribution of the FLUXNET sites selected.

3.1.1. DESCRIPTION OF THE IN-SITU DATA

Model outputs are evaluated against sites selected from FLUXNET 2015 database. The FLUXNET database contains data of ecosystem CO_2 fluxes obtained with the eddy-covariance technique. This well-established technique provides GPP data from the post-processing of the direct measurement of net ecosystem CO_2 exchange. FLUXNET integrates data from regional networks, international projects and field-sites of research institutes and provides a highly standardized data treatment and data analysis (including uncertainty estimations) for measuring sites distributed globally. These data have been extensively used for the development and evaluation of ecological models at regional or global scale (Balzarolo et al., 2014).

The FLUXNET GPP data are well suited to be used as validation product for several reasons: (i) they are available at both very high time resolution (half-hourly) and aggregated at longer time step (daily to annual), (ii) are available for multiple years (up to >10 years for the most intensively studied sites), (iii) data are provided with uncertainty estimations (http://fluxnet.fluxdata.org/data/fluxnet2015-dataset/data-processing/) , and (iv) sites are available globally and for all types of terrestrial ecosystems (e.g. forests, grasslands, croplands, wetlands, tundra). FLUXNET has been established in 1998 (Baldocchi, 2008) and since then techniques have improved and different database version have been produced. In this project, we use the latest version (FLUXNET 2015, http://fluxnet.fluxdata.org/data/fluxnet2015-dataset/). About 200-250 GPP site are available now.

3.1.2. SITE SELECTION

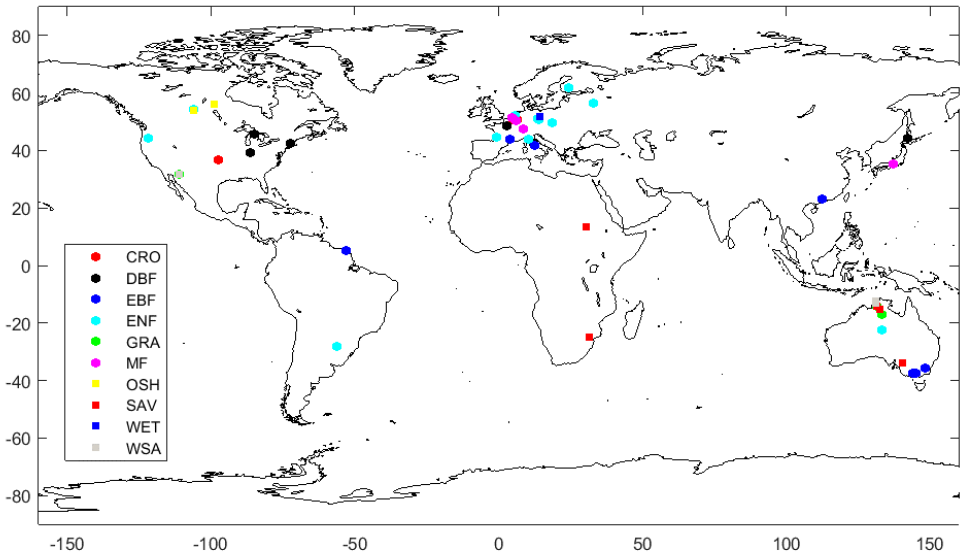

Figure 1 shows the geographical distribution of the FLUXNET sites selected as ideal sites for the validation of GPP model simulations. These sites are ideal because they have:

- Good data quality. GPP data quality was checked by following the standardized methodology defined in the FLUXNET (Reichstein et al., 2005; Papale et al., 2006). Only the sites containing at least one year of carbon flux data of good quality and only daily data with a percentage of gap-filled half hours less than 15% were used in this analysis.
- A large homogenous footprint area at least 1 km x 1 km spatial resolution to ensures reliable comparisons between in-situ and remotely sensed data. The site homogeneity was visually described by using Google Earth high-resolution images.

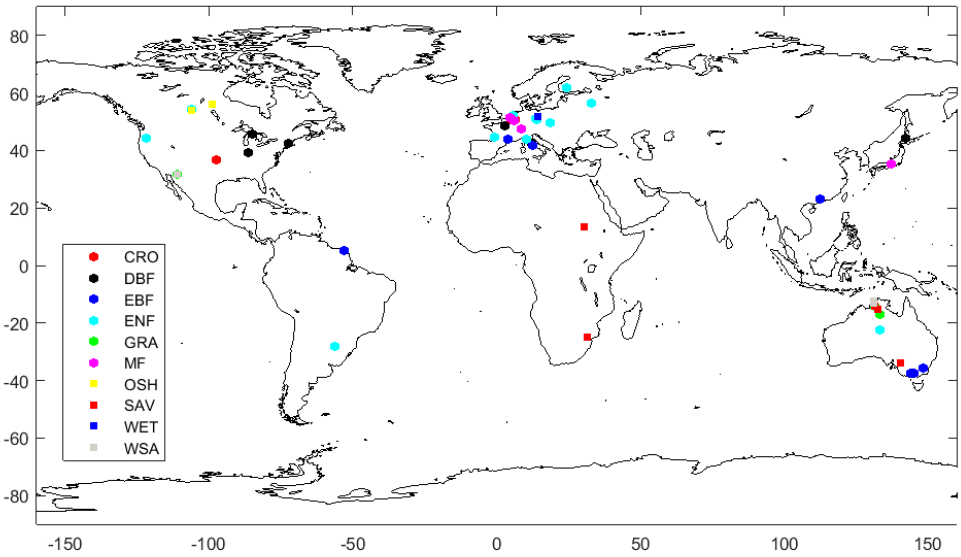

Figure 1: Geographical distribution of the FLUXNET 2015 sites selected for the validation of the model outputs. ENF—Evergreen Needle leaf Forest; EBF—Evergreen Broadleaf Forest; DBF—Deciduous Broadleaf Forest; MF—Mixed Forest; CRO—Cropland; GRA—Grassland; SAV—Savanna; WSA—Woody Savanna; and OSH—Open Shrubland.

3.1.3. STATISTICAL METRICS

The performance of the models is evaluated by comparing the simulated values of GPP by the model with GPP values obtained from flux sites. The performance analysis included the coefficient of determination (R^2), to evaluate the phase correlation, the absolute root mean square error (RMSE) and mean absolute error (MAE) to analyze how the individual errors were distributed and the percentage bias (pBias) to measure the average tendency of the simulated values to be larger or smaller than their observed ones.

We calculated the above-cited errors in the following manner:

$$R^2 = \frac{\left[\sum_{i=1}^{N}(Pi-\overline{P})(Oi-\overline{O})\right]^2}{\sum_{i=1}^{N}(Pi-\overline{P})^2\sum_{i=1}^{N}(Oi-\overline{O})^2}$$

$$RMSE = \sqrt{\frac{1}{N}\sum_{i=1}^{N}(Pi - Oi)^2}$$

$$MAE = \frac{1}{N}\sum_{i=1}^{N}|Pi - Oi|$$

$$pBIAS = 100 * \frac{\sum_{i=1}^{N}(Pi - Oi)}{\sum_{i=1}^{N}Oi}$$

where O_i is daily averaged measured fluxes and P_i daily-simulated fluxes; $\overline{O}$ and $\overline{P}$ denote their means.

The RMSE is the residual standard deviation and bias the residual mean. A value of RMSE close to zero indicates that simulations are close to the measured data. Positive values of bias indicate average overestimation by the simulation and negative values indicate average underestimation. The MAE is a simple difference between predicted and observed values. The pBIAS measures the average tendency of the simulated values to be larger or smaller than their observed ones. The optimal value of pBIAS is 0.0, with low-magnitude values indicating accurate model simulation. Positive values indicate overestimation bias, whereas negative values indicate model underestimation bias. In addition to these statistical metrics, the slope of the regression line that represent the rate of change in y as x cahnges as been considered.

The statistical metrics were computed for seasonal (considering mean values over 10 day time window matching the time resolution of model outputs) and annual validation (considering mean annual values calculated only for the years for which the remote sensed product matches observations).

The following metrics were be tested:

1. Seasonal variability in GPP at 10 days time scale (considering mean values over 10 days time window that matched the time resolution of models outputs).
2. Between-sites differences in average annual GPP based on different ecosystems (spatial variation).
3. Between-year variability based on different ecosystems (interannual variability).

All statistics were computed only for the years for which the remote sensed product matches observations.

Moreover, the model capability to describe the Rg-GPP response curve was tested by comparing the observed and modeled GPP responses to shortwave incoming global radiation.

In addition, the goodness of the meteorological forcing were evaluated with in-situ data by linear correlation analysis and $R^2$and RMSE statistical metrics.

CHAPTER 4 RESULTS OF THE VALIDATION AT GLOBAL SCALE

4.1. PERFORMED ACTIVITIES

In this session are reported the results of the GPP validation at global scale. We evaluated the model outputs provided by ICL over FLUXNET sites.

For the sake of clarity, we don't present all results of seasonal and yearly variation for each site but only a synthetic view of the statistical analyses. Statistical analyses were computed by separating data sets concerning the main ecosystems: ENF—Evergreen Needleleaf Forest; EBF—Evergreen Broadleaf Forest; DBF—Deciduous Broadleaf Forest; MF—Mixed Forest; CRO—Cropland; GRA—Grassland; SAV—Savanna; WSA—Woody Savanna; and OSH—Open Shrubland.

Results of the GPP verification at global scale are presented in section 4.2, 4.3 and 4.4.

In section 4.4 the results of the GPP-Rg response analysis are reported and in section 4.5 the results of meteo forcing validation.

4.2. SIMULATION PERFORMANCE BY ECOSYSTEMS

Table 2 reports the mean performance values of the simulated 10 days GPP for the ECMWF and LST model runs, pooled by ecosystems. In this analysis ECMWF model simulations were evaluated against in-situ data of 58 sites and LST simulations were evaluated against 46 sites. Overall, the use of LST reduces the magnitude of biases for most of ecosystems relative to the use of ECMWF data. This could be related to the sensitivity of the model to air temperature used as imput. The ECMWF model simulation tends to overestimate GPP for all ecosystems while the LST model simulation underestimates GPP of WSA, GRA, SAV, EBF and ENF. Both simulations markedly underestimate GPP of WET. The ECMWF model simulation markedly over or underestimate the seasonal variation of GPP for all PFT compared to LST model.

Figure 2 shows the performances of ECMWF and LST model simulations for the same number of sites. This analysis confirms that the LST model simulation clearly reduces the bias for most PFTs. However, seasonal GPP of WET and OSH is consistently overestimated by both models. For WET, the mismatch between the model simulations and in-situ data could be related to the presence of water that impact on surface spectral response. For open shrublands, this is most likely because the model does not take into account the impact of soil moisture on LUE (Stocker et al., 2018).

PFT	Slope (-)	Slope_err (-)	R^2 (-)	p-value (-)	MAE (gC m^{-2} d^{-1})	RMSE (gC m^{-2} d^{-1})	pBIAS (%)
ECMWF							
ENF	0.83	0.03	0.58	0.00	1.85	2.33	16.69
WSA	1.00	0.03	0.78	0.00	1.11	1.38	24.90
SAV	1.00	0.05	0.51	0.00	1.20	1.57	10.83
GRA	0.77	0.04	0.68	0.00	1.32	1.58	50.00
EBF	0.96	0.03	0.39	0.00	2.14	2.68	6.66
MF	0.72	0.02	0.68	0.00	2.05	2.73	38.16
CRO	0.77	0.06	0.46	0.00	3.06	3.83	40.18
OSH	0.54	0.02	0.71	0.00	1.92	2.22	98.38
WET	0.58	0.02	0.80	0.00	2.60	2.96	104.63
DBF	0.68	0.02	0.70	0.00	3.19	3.80	54.15
LST							
WSA	1.40	0.10	0.57	0.00	1.30	1.61	-21.70
GRA	1.27	0.08	0.87	0.00	1.66	2.12	-14.50
SAV	2.39	0.36	0.35	0.00	1.84	2.12	-27.85
EBF	1.17	0.04	0.36	0.00	1.97	2.33	-11.96
MF	0.83	0.02	0.68	0.00	1.50	2.04	22.83
CRO	1.00	0.06	0.52	0.00	2.13	2.88	12.95
OSH	0.67	0.07	0.45	0.00	0.88	1.10	56.73
ENF	1.04	0.04	0.53	0.00	1.65	2.05	-7.54
DBF	0.91	0.04	0.63	0.00	2.16	2.65	15.06
WET	0.49	0.03	0.64	0.00	2.34	2.59	116.00

Table 2: Mean performance values of the simulated 10 days GPP for the two model runs, pooled by ecosystems.

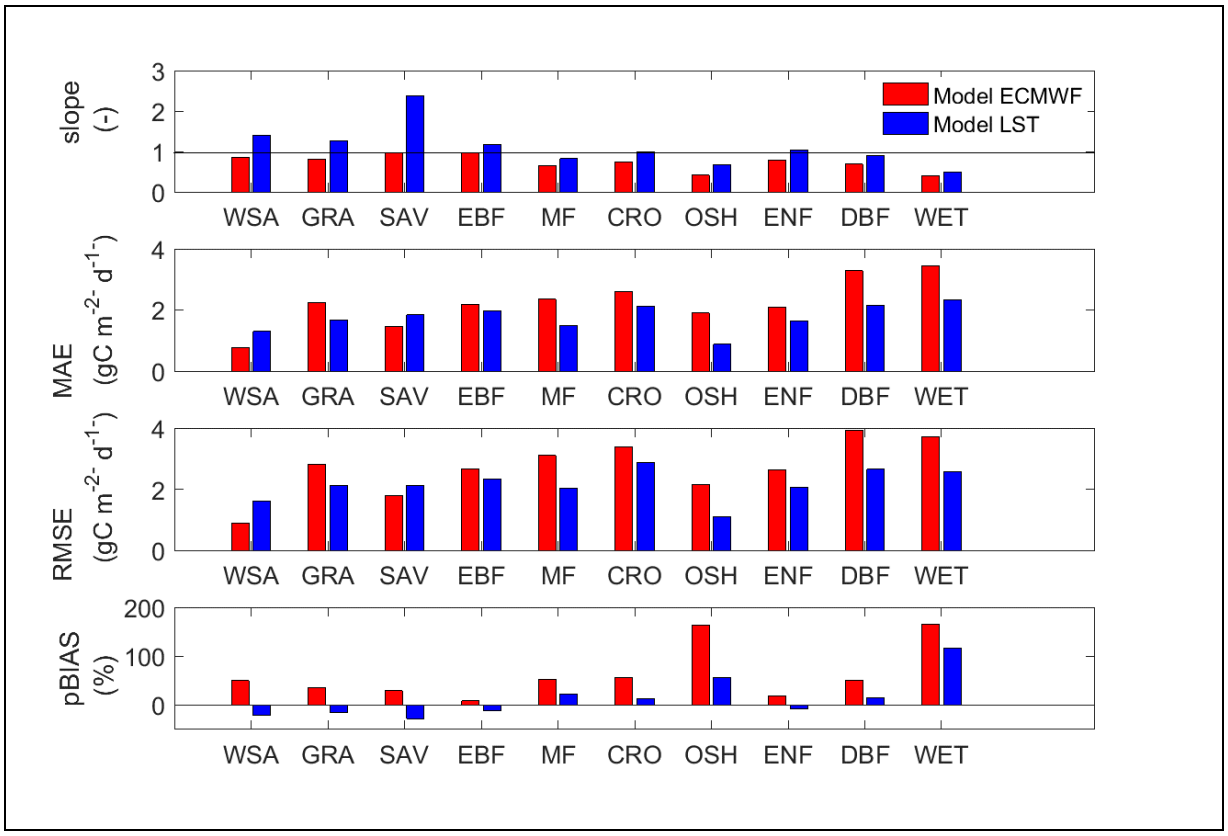

Figure 2: Performances of ECMWF and LST model simulations of 10 days GPP for the same number of sites and across ecosystems on a site × year basis: (from top to bottom) slope, MAE, RMSE and pBIAS, respectively.

4.3. ANNUAL VALIDATION

The first part of this section carries out the validation of in-situ observed and modelled spatial variations (among sites) in annual GPP for both model simulations. The second part focuses on the model's ability to reproduce between-year variability (interannual variability).

The ECMWF model simulations were evaluated against in-situ annual GPP data of 58 sites and LST simulations were evaluated against 46 sites.

Table 3, Figure 3 and Figure 4 report the results of annual validation for ECMWF and LST model simulations respectively. Overall the magnitude of pBIAS for the LST simulations is smaller than for ECMWF. The slope values for LST simulations are generally greater than one indicating the LST model tends to underestimate the annual GPP. Both simulations show quite similar slopes in predicting GPP annual variability of DBF. The ECMWF simulation describes quite well the GPP annual variability of EBF, ENF and SAV. A poor performance is found for WET that shows a quite large error around the correlation. The LST simulation shows quite good performance in predicting GPP annual variability for MF while tends to overestimate the annual GPP of EBF and ENF. The LST simulation tends to underestimate the GPP annual values of SAV and WSA. It shows a very good performance for CRO but the error around the correlation.

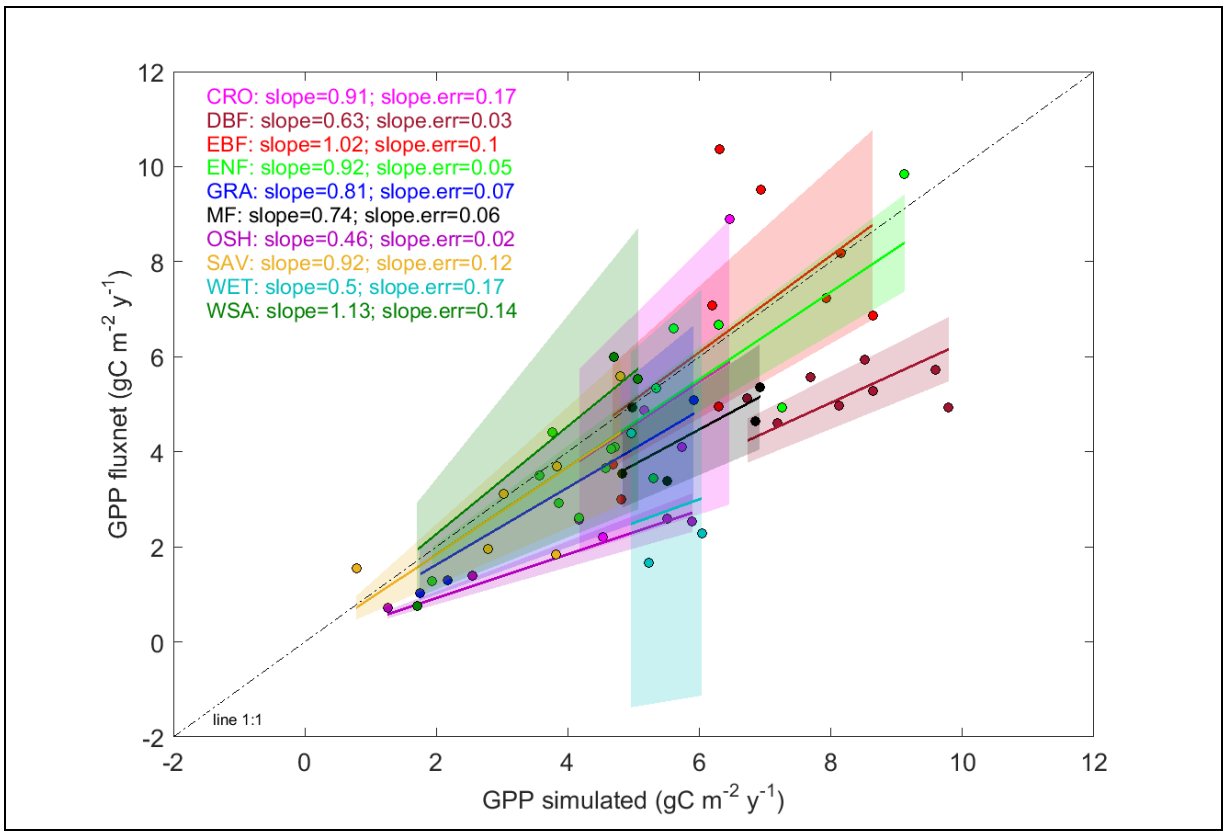

Figure 3: Comparison of in-situ observed and modelled spatial variations in annual GPP for ECMWF model simulation, pooled by ecosystems. The area represents the 95% confidence bounds for the slope of fitted line.

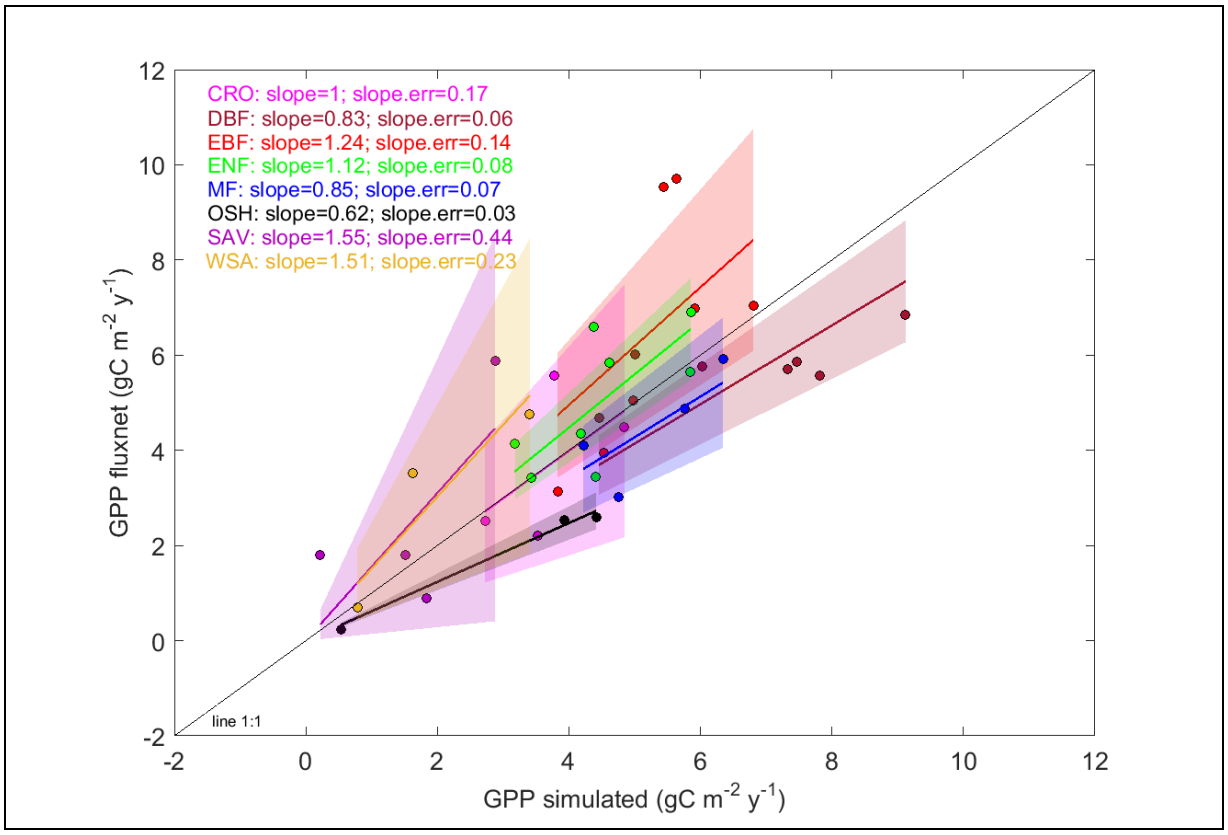

Figure 4: Same as in Fig. 3, expected for LST model simulations.

PFT	Slope (-)	Slope_err (-)	R^2 (-)	p-value (-)	MAE (gC m^{-2} d^{-1})	RMSE (gC m^{-2} d^{-1})	pBIAS (%)
EMCWF							
ENF	0.92	0.05	0.78	0.00	0.87	1.07	10.70
WSA	1.13	0.14	0.97	0.01	0.90	0.96	-6.60
SAV	0.92	0.12	0.55	0.00	0.77	0.99	7.30
GRA	0.81	0.07	0.99	0.01	0.81	0.81	32.70
EBF	1.02	0.10	0.33	0.00	1.57	1.93	-1.60
MF	0.70	0.03	0.33	0.00	1.80	1.84	42.50
CRO	0.91	0.17	0.81	0.01	1.66	1.82	15.10
OSH	0.46	0.02	0.99	0.00	1.99	2.31	109.70
WET	0.50	0.17	0.28	0.10	2.63	3.01	94.80
DBF	0.65	0.02	0.37	0.00	2.75	2.84	51.70
LST							
WSA	1.51	0.23	0.83	0.02	1.11	1.34	-35.20
SAV	1.55	0.44	0.46	0.04	1.45	1.77	-37.90
EBF	1.24	0.14	0.44	0.00	1.54	2.25	-18.20
MF	0.85	0.07	0.67	0.00	0.79	1.00	17.60
CRO	1.00	0.17	0.34	0.01	0.92	1.13	0.70
OSH	0.62	0.03	0.98	0.00	0.90	1.15	59.00
ENF	1.12	0.08	0.48	0.00	0.84	1.08	-11.10
DBF	0.83	0.06	0.49	0.00	1.32	1.54	16.70

Table 3: Results of the validation of in-situ observed and modelled spatial variations in annual GPP for both model simulation, pooled by ecosystems.

Table 4 shows the results of the model validation at the multi-annual time scale. This analysis focuses on the model's ability to reproduce between-year variability and the results are summarized within ecosystems. Overall, the LST model tends to reduce the magnitude of bias for most of biomes (Table 5: MF, CRO, OSH, ENF and DBF) , except for WET. Generally, the LST model underestimates the interannual variability of GPP while ECMWF model overestimates it. The ECMWF simulation describes quite well the GPP interannual variability of EBF, WSA and SAV. The LST simulation shows quite good performance in predicting GPP interannual variability for DBF and MF while tends to overestimate GPP interannual variability of EBF and ENF. The LST shows a good performance for CRO.

PFT	Slope (-)	Slope_err (-)	R^2 (-)	p-value (-)	MAE (gC m^{-2} d^{-1})	RMSE (gC m^{-2} d^{-1})	pBIAS (%)
ECMWF							
ENF	0.88	0.03	0.68	0.00	1.15	1.40	14.30
WSA	1.10	0.07	0.95	0.00	0.90	1.05	-1.00
SAV	0.97	0.07	0.58	0.00	1.06	1.32	4.70
GRA	0.83	0.04	0.96	0.00	0.81	0.94	29.70
EBF	0.98	0.06	0.30	0.00	1.86	2.27	1.30
MF	0.71	0.02	0.62	0.00	1.81	2.03	39.80
CRO	0.71	0.05	0.41	0.00	1.80	2.08	43.50
OSH	0.47	0.03	0.91	0.00	1.44	1.84	102.30
WET	0.60	0.11	0.57	0.00	2.37	2.85	76.40
DBF	0.66	0.02	0.78	0.00	2.74	2.96	51.20
LST							
WSA	1.39	0.11	0.89	0.00	0.88	1.10	-27.30
SAV	1.16	0.31	0.18	0.00	1.31	1.58	-29.90
EBF	1.11	0.06	0.58	0.00	1.05	1.52	-9.20
MF	0.89	0.05	0.21	0.00	0.98	1.22	11.20
CRO	0.93	0.09	0.37	0.00	1.00	1.32	8.40
OSH	0.63	0.03	0.96	0.00	0.77	1.03	51.50
ENF	1.08	0.05	0.58	0.00	0.87	1.20	-7.40
DBF	0.82	0.04	0.22	0.00	1.34	1.75	18.60
WET	0.47	0.04	0.99	0.00	2.46	2.47	114.30

Table 4: Results of the interannual variability, pooled by PFT.

4.4. ENVIRONMENTAL CONTROLS OF FLUXES

Figs. 5-12 show some examples of the seasonal GPP trend of different PFTs. Overall, the ECMWF simulation tends to overestimate GPP for all sites. The LST model simulation follows the seasonal GPP dynamics observed by EC for all sites. ECMWF forcing shows a good correlation with the in-situ Ta observation (see below, Figs. 20-28) for different sites while LST forcing (see below, Figs. 29-34) tends to overestimate in-situ. Soil and air temperature play a fundamental role in the partitioning algorithm used to calculated in-situ respiration and therefore estimate GPP. An overestimation of temperature could lead to an overestimation of GPP for most of ecosystems. fAPAR is a good proxy of deciduous forest (DBF), grasslands (Fig. 10) and savannas. Therefore the EMCWF model capture quite well the seasonal dynamics of DBF too (Fig. 5). However, LST improve the estimation of seasonally variability of ENF (Fig. 6) and EBF (Fig. 7) because carbon dynamics of evergreen vegetation is not related to vegetation greenness. Therefore fAPAR is not a good proxy of the phenology of these ecosystems. Other remote sensed vegetation index like Enanched Vegetation Index (EVI) should be tested for describing the phenology of evegreen forests. In addition, the model overestimates GPP of EBF located in the Mediterranean region (Fig. 7). This is due to neglect of the soil moisture effect in the model. In addition the reduction of GPP related to drough

is not sensed by canopy greeneess and it is assumable that fAPAR is sensible to changes in carbon flux during drough periods. For the EBF site in Tropical region (Fig. 8) the model generally underestimates GPP. This might be due to the extremely cloudy conditions that leads to underestimation of fAPAR and the quality of in-situ data. Regarding CRO sites (Fig. 9), the disagreement between in-situ data and model predictions could be due to several aspects. First, the cropland phenology could be not well described by in-situ data due to the small flux footprint compared to satellite pixels. The fAPAR data could show "green-up" too early or the in-situ GPP data are biased because the partitioning algorithm is underestimating Reco during the early growth phase. Secondly, the impact of the management that it is not taken into account by the model. Finally, for open shrublands, this is most likely because the model does not take into account the impact of soil moisture on LUE (Stocker et al., 2018).

Plots in Figs. 13-20 show the GPP response curves global radiation (Rg) for the same sites presented in Figs. 5-12. All simulations present some limitation in describing ecological functions controlling GPP for all sites. The model simulations tend to overestimate the slopes for the investigated ecological functions for the deciduous broadleaf forest site (Fig. 13) and for the cropland (Fig. 17).

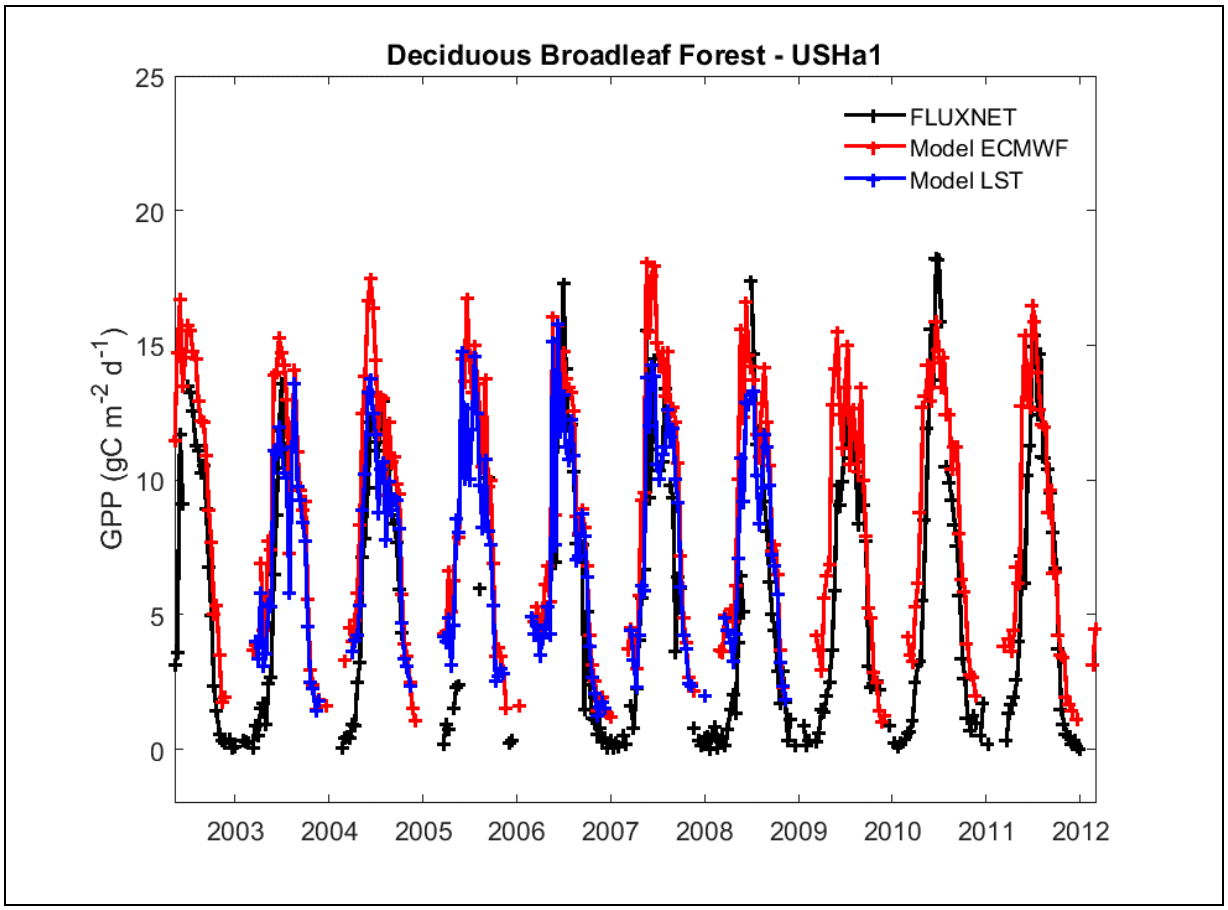

Figure 5: Annual cycle of the daily GPP for deciduous broadleaf forest site in US. ECMWF simulation is in red, LST simulation in blue while black line represents in-situ measured data.

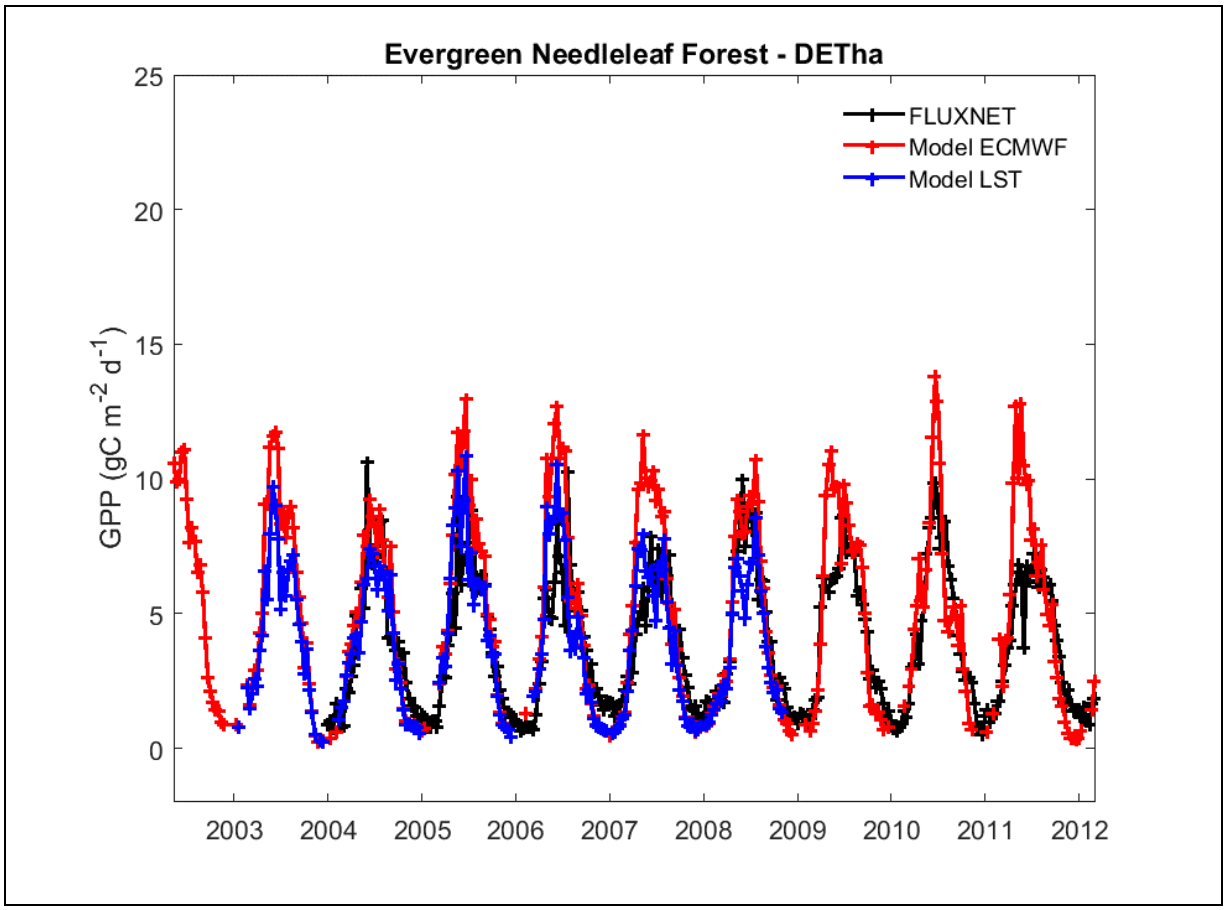

Figure 6: Annual cycle of the daily GPP for an evergreen needle leaf forest site in Germany. ECMWF simulation is in red, LST simulation in blue while black line represents in-situ measured data.

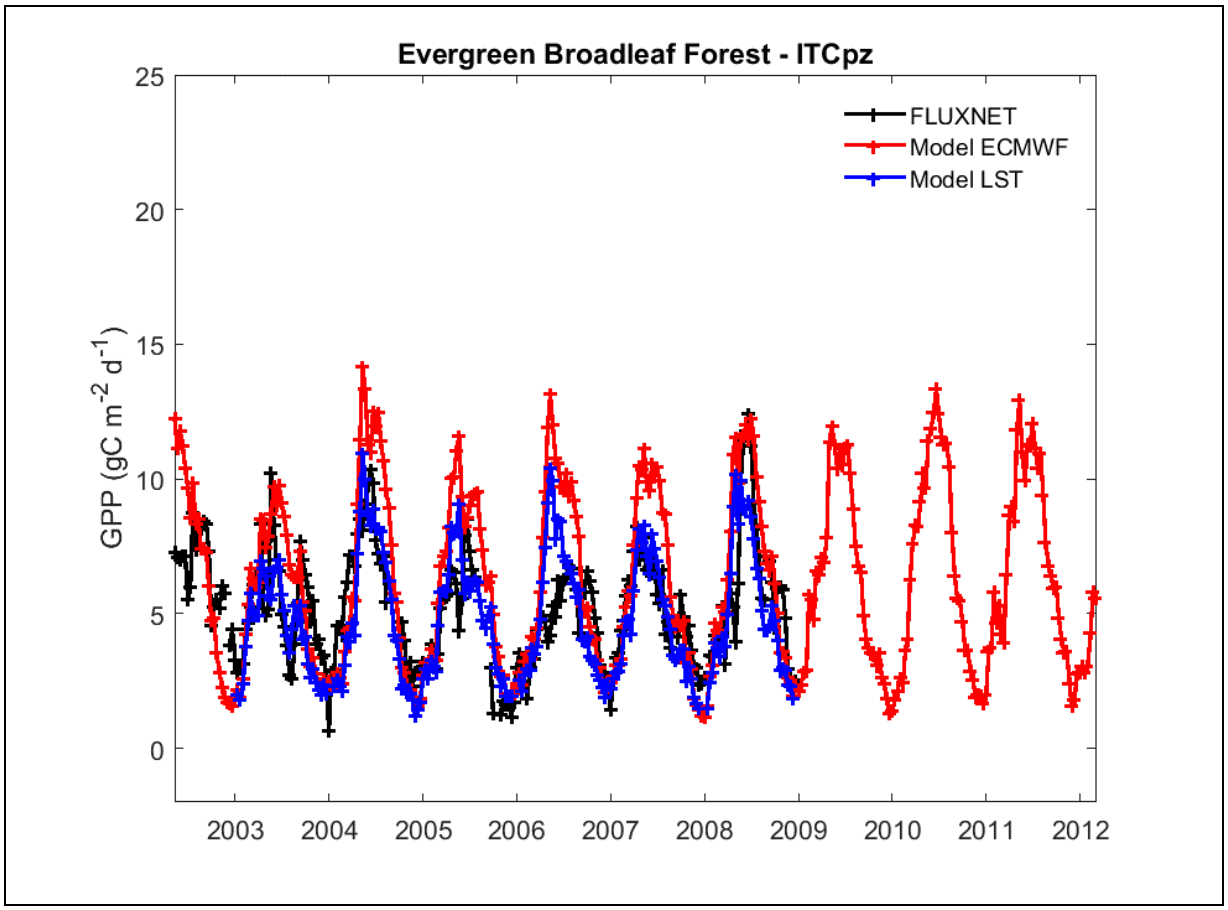

Figure 7: Annual cycle of the daily GPP for an evergreen broadleaf forest site in Italy. ECMWF simulation is in red, LST simulation in blue while black line represents in-situ measured data.

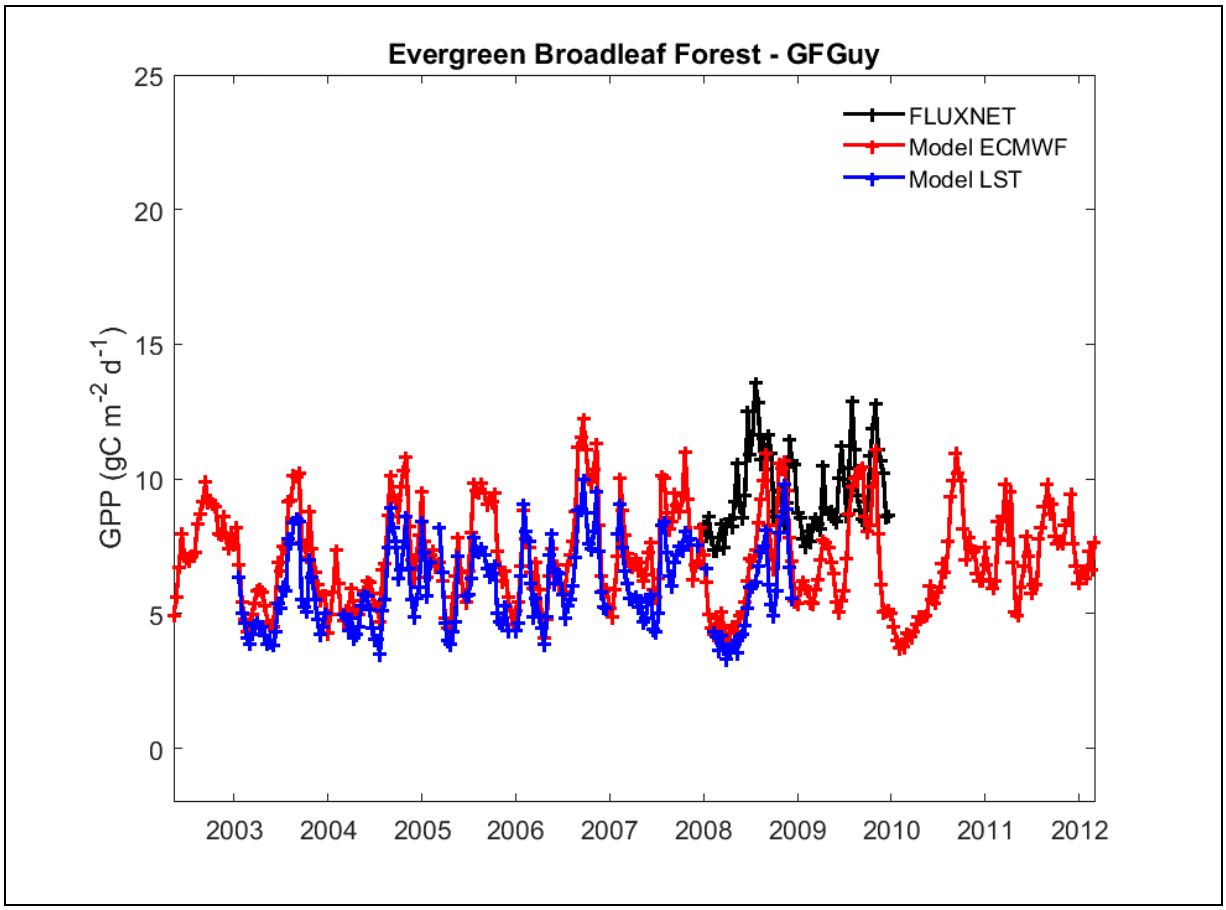

Figure 8: Annual cycle of the daily GPP for an evergreen broadleaf forest site in French Guyana. ECMWF simulation is in blue, LST simulation in black while magenta line represents in-situ measured data.

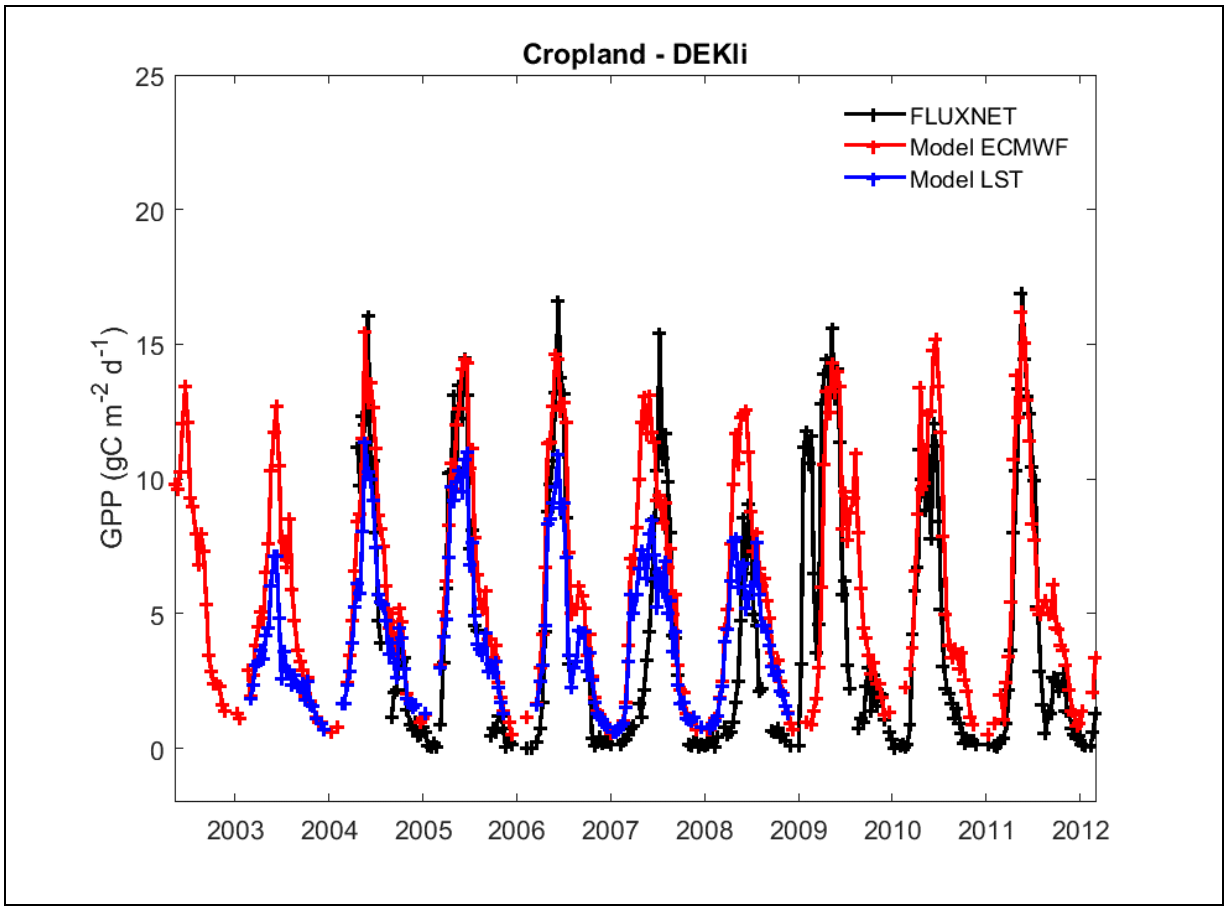

Figure 9: Annual cycle of the daily GPP for cropland site in Germany. ECMWF simulation is in blue, LST simulation in black while magenta line represents in-situ measured data.

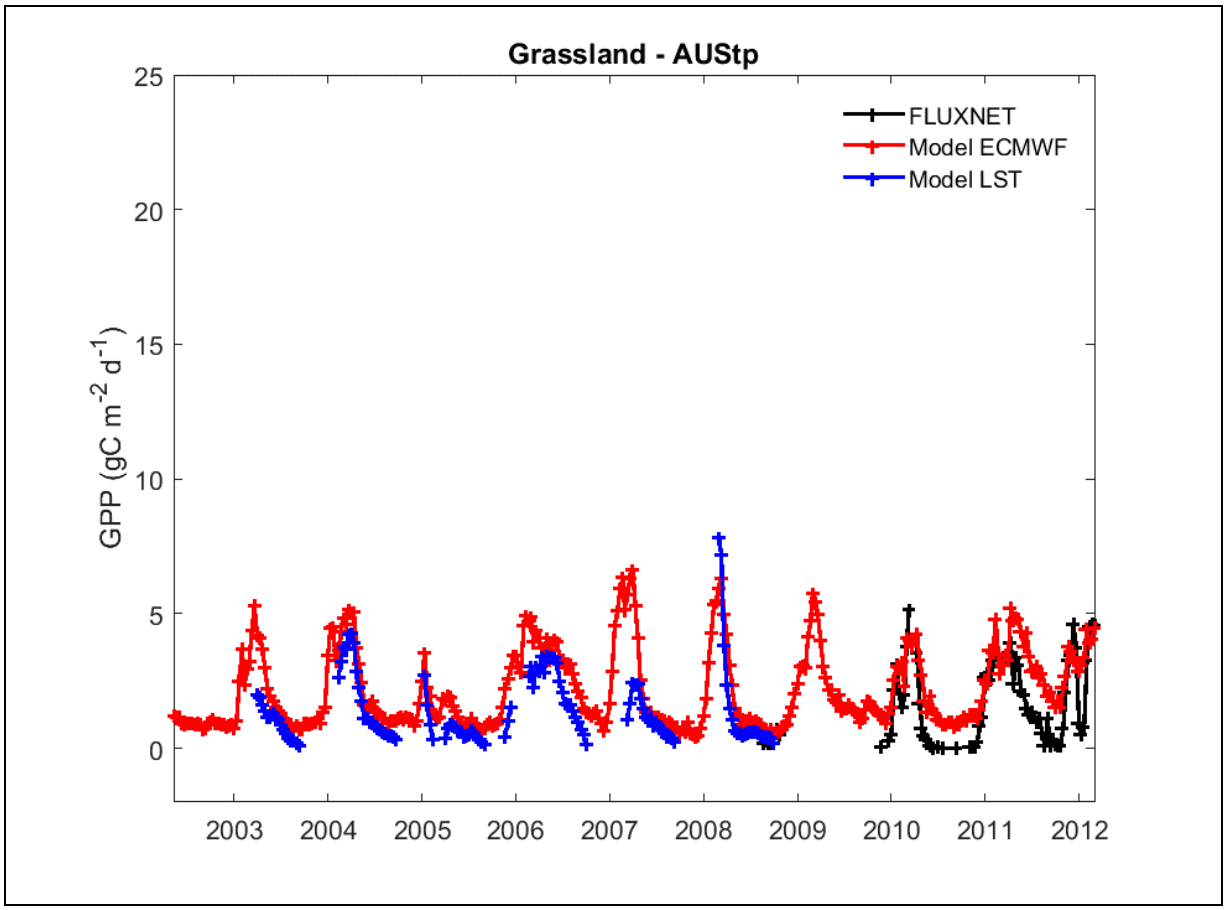

Figure 10: Annual cycle of the daily GPP for grassland site in Australia. ECMWF simulation is in blue, LST simulation in black while magenta line represents in-situ measured data.

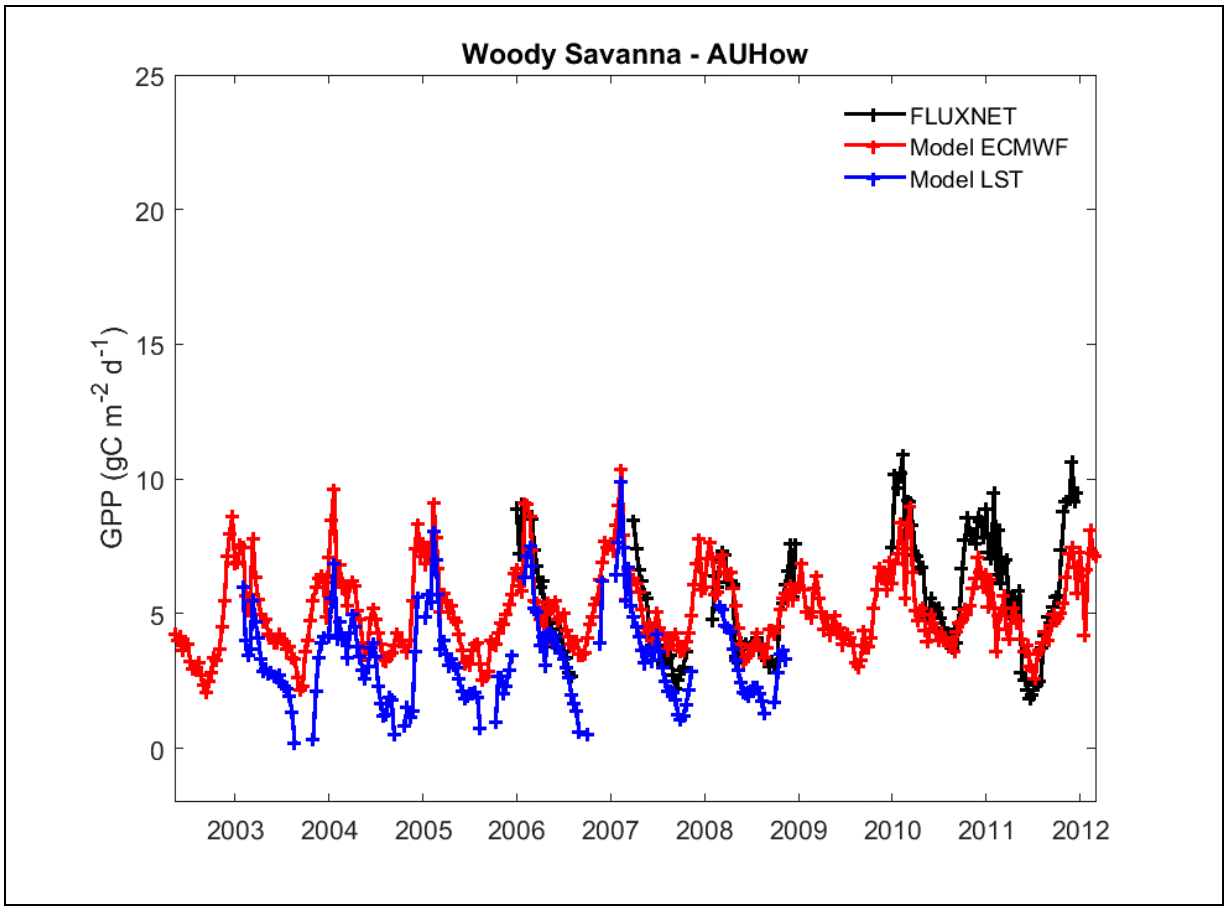

Figure 11: Annual cycle of the daily GPP for a woody savanna site in Australia. ECMWF simulation is in blue, LST simulation in black while magenta line represents in-situ measured data.

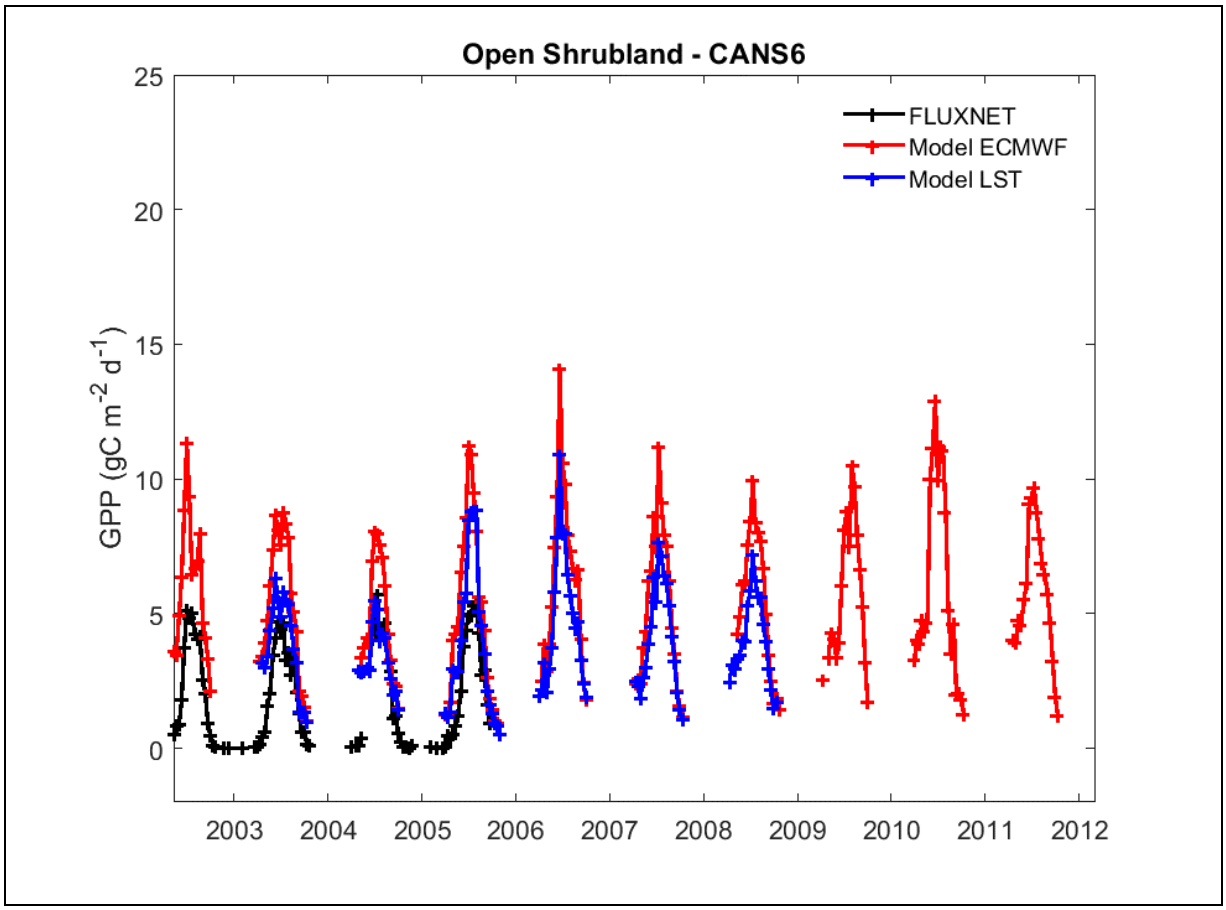

Figure 12: Annual cycle of the daily GPP for an open shrubland site in US. ECMWF simulation is in blue, LST simulation in black while magenta line represents in-situ measured data.

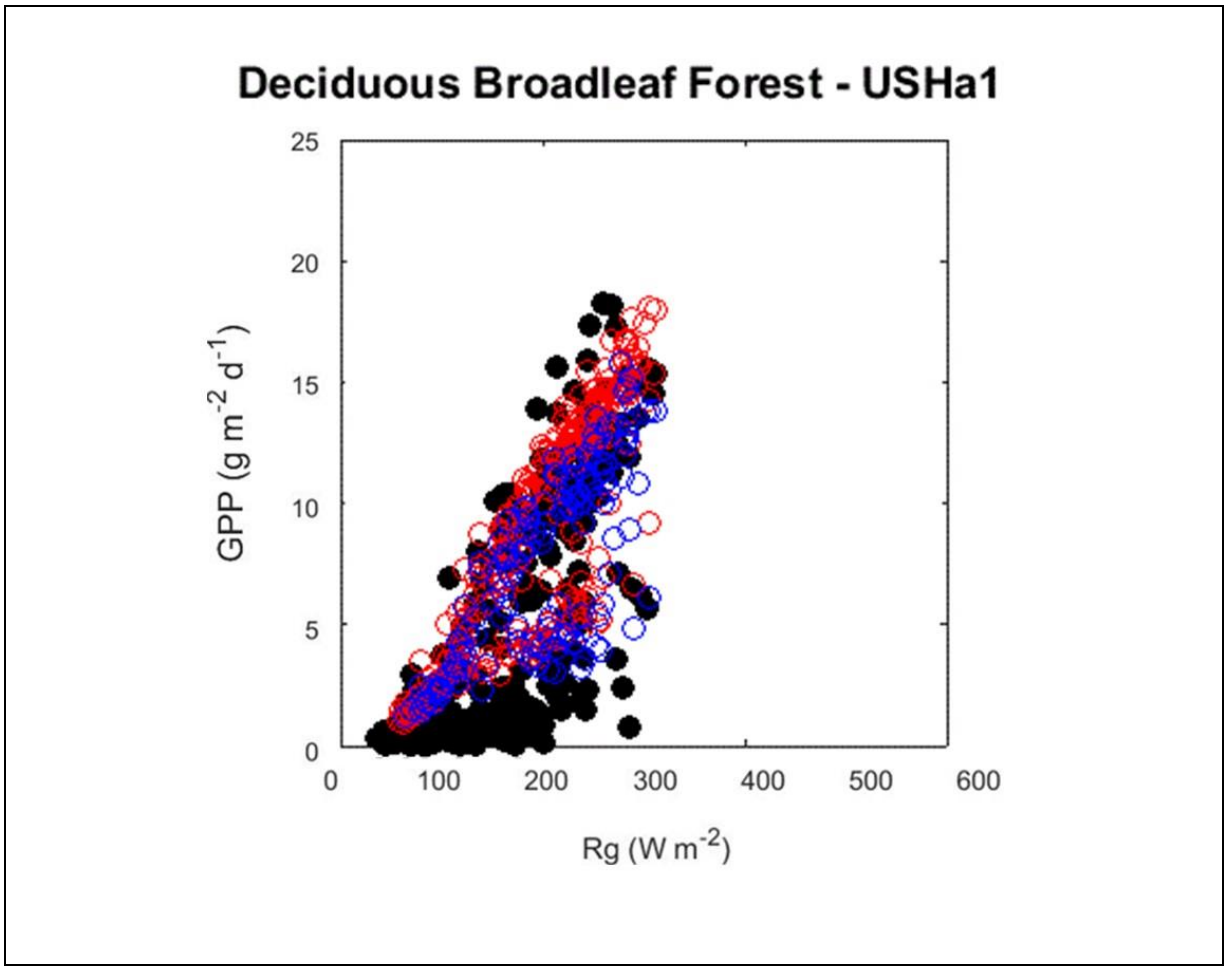

Figure 13: GPP response curves to global radiation (Rg) for a deciduous broadleaf forest site in US. ECMWF simulation is in red, LST simulation in blue while black dots represents in-situ measured data.

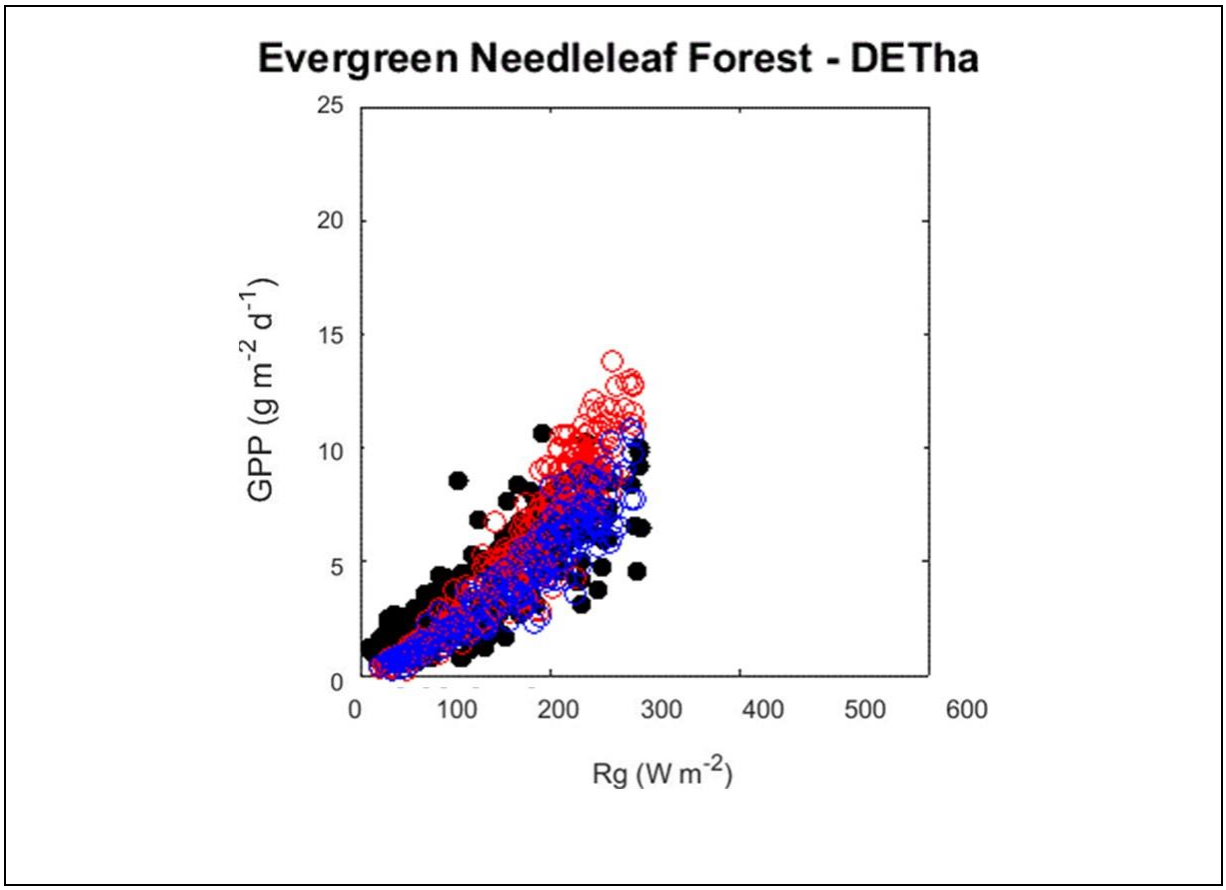

Figure 14: GPP response curves to global radiation (Rg) for an evergreen needle leaf forest site in Germany. ECMWF simulation is in red, LST simulation in blue while black dots represents in-situ measured data.

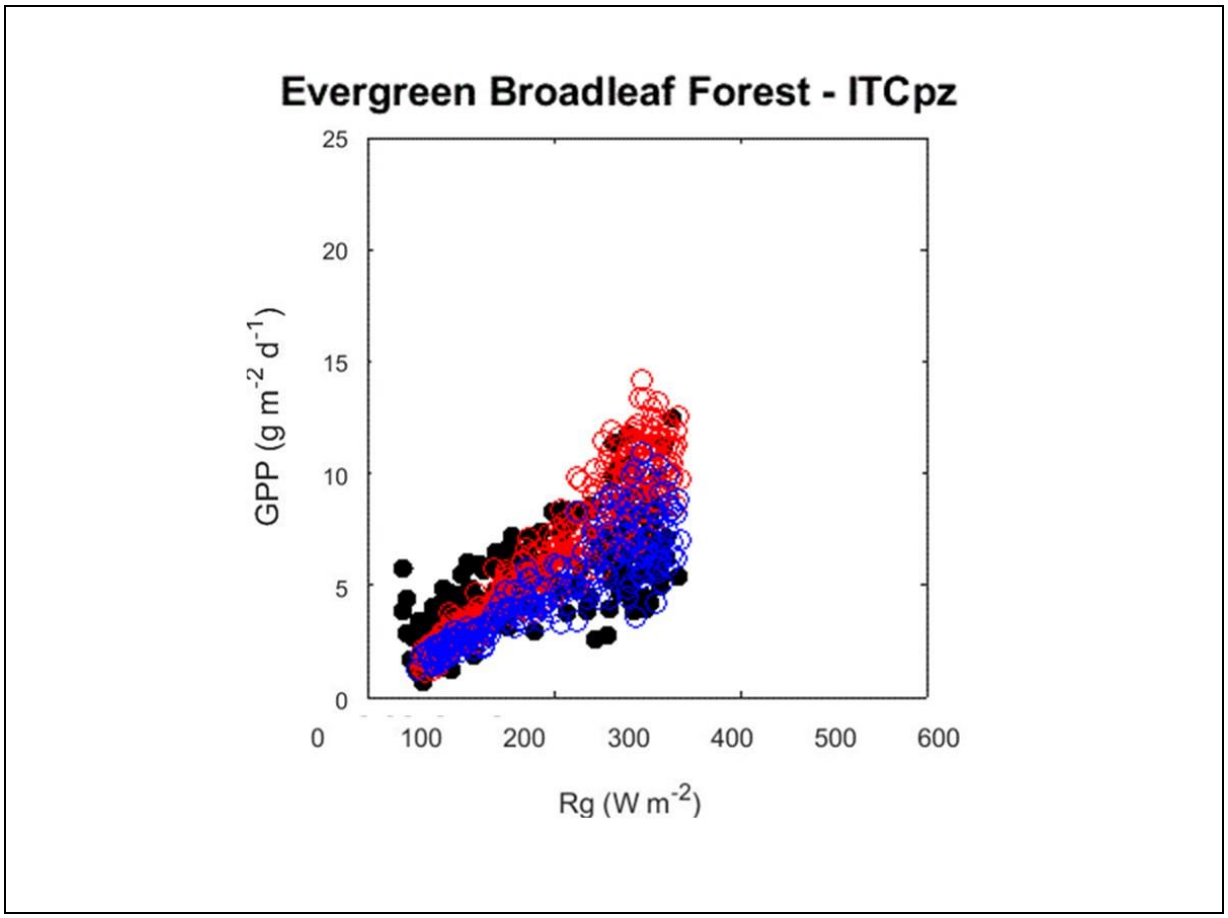

Figure 15: GPP response curves to global radiation (Rg) for an evergreen broadleaf forest site in Italy. ECMWF simulation is in red, LST simulation in blue while black dots represents in-situ measured data.

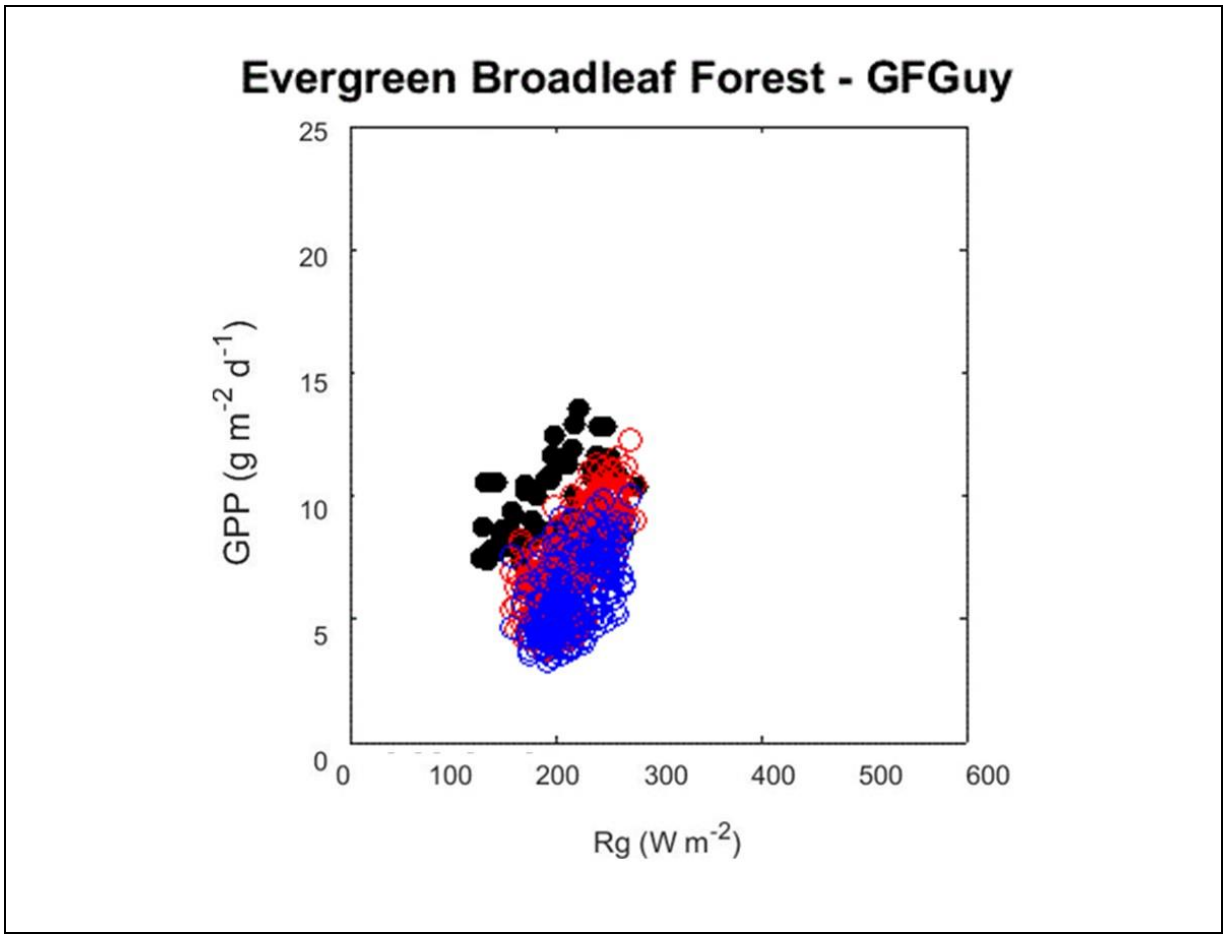

Figure 16: GPP response curves to global radiation (Rg) for an evergreen broadleaf forest site in French Guyana. ECMWF simulation is in red, LST simulation in blue while black dots represents in-situ measured data.

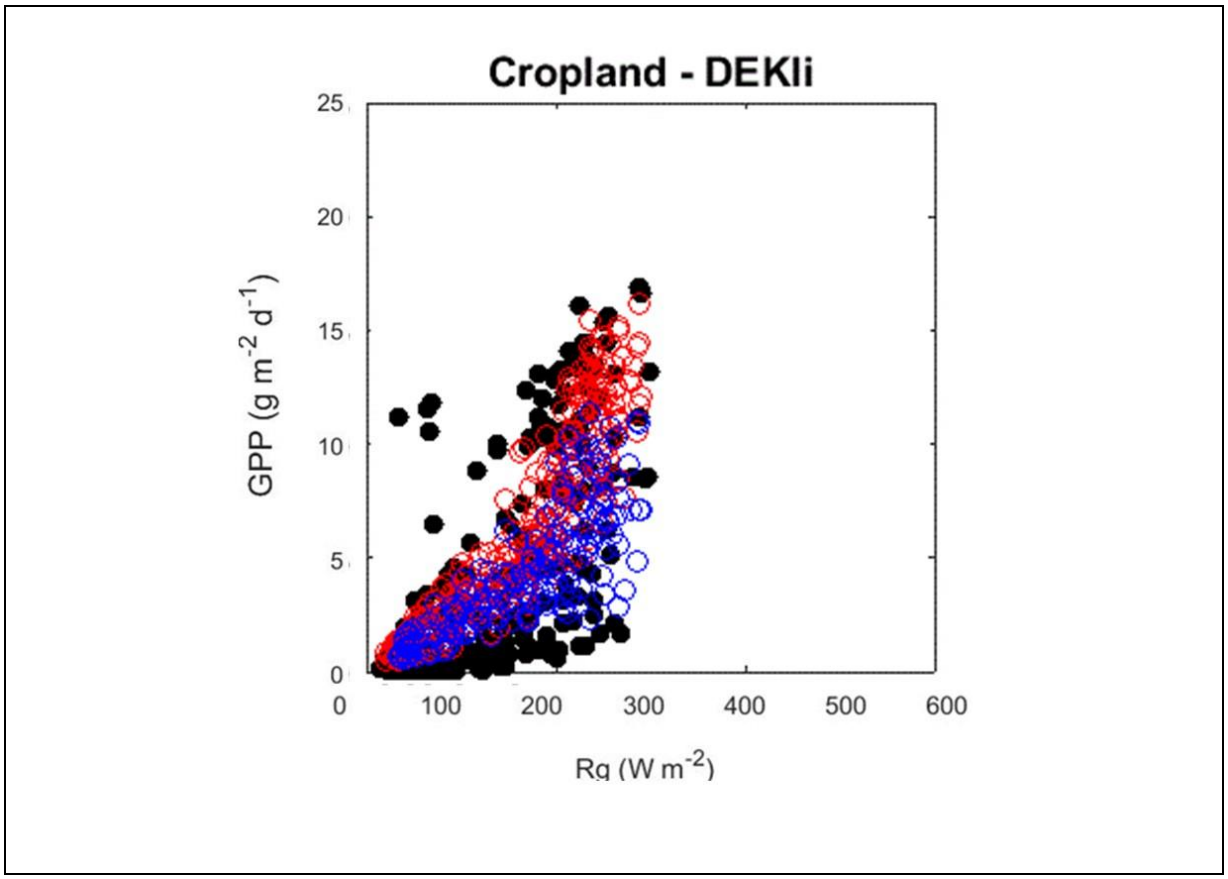

Figure 17: GPP response curves to global radiation (Rg) for a cropland site in Germany. ECMWF simulation is in red, LST simulation in blue while black dots represents in-situ measured data.

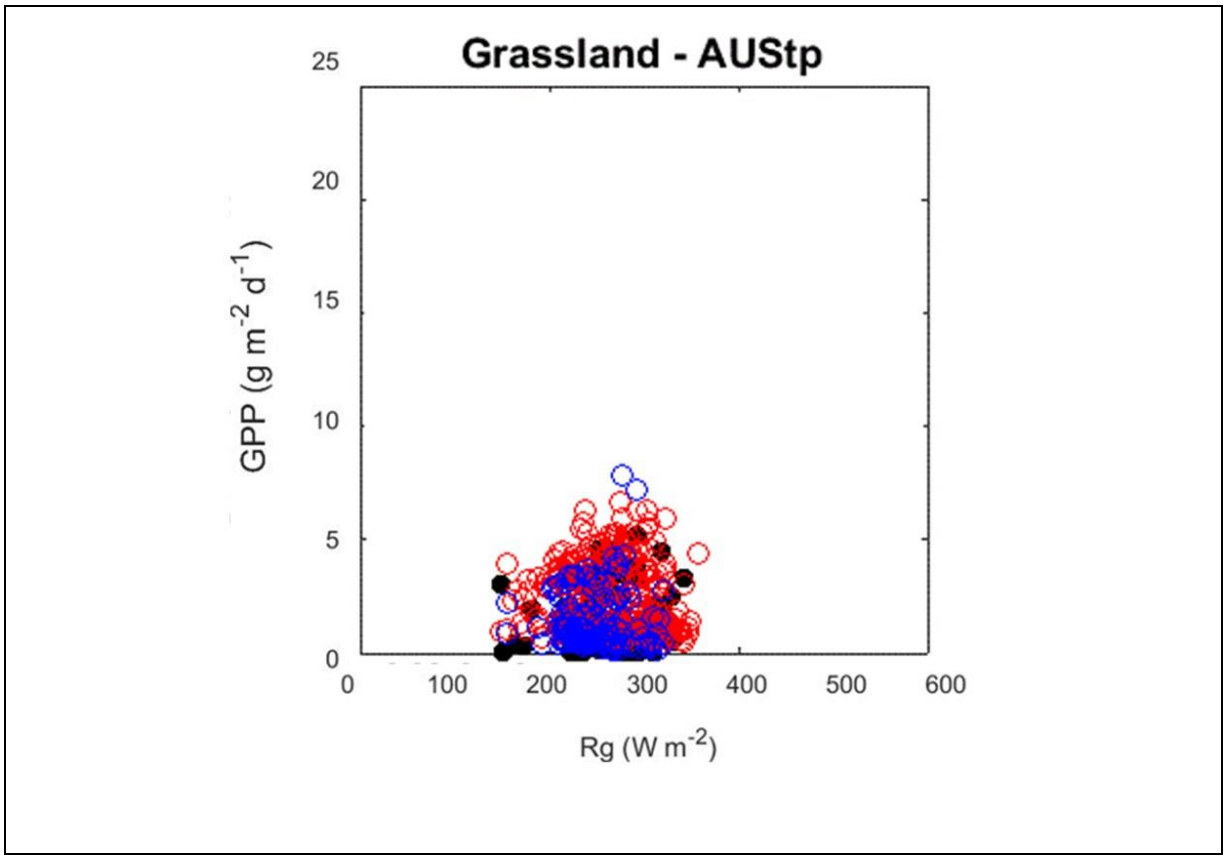

Figure 18: GPP response curves to global radiation (Rg) for a deciduous broadleaf forest site in US. ECMWF simulation is in red, LST simulation in blue while black dots represents in-situ measured data.

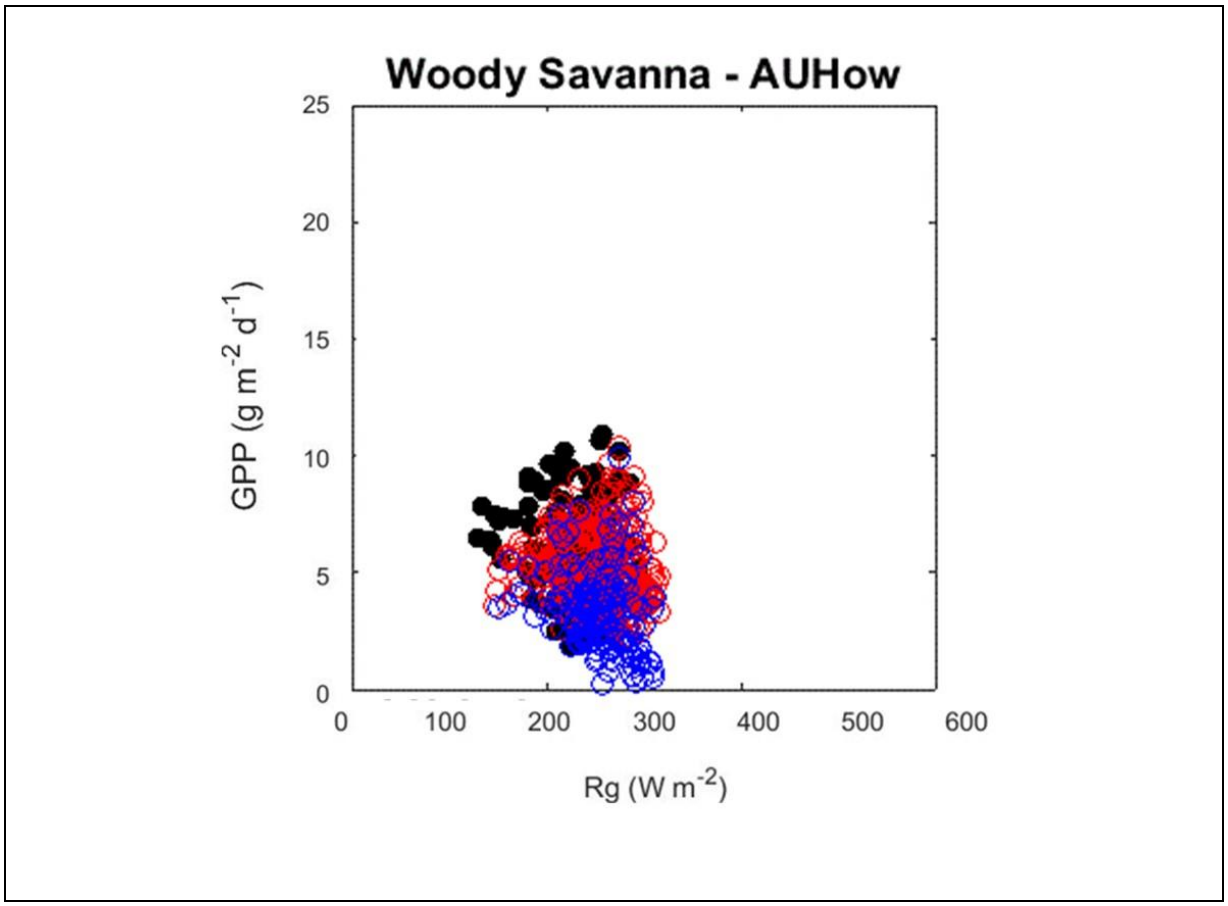

Figure 19: GPP response curves to global radiation (Rg) for a woody savanna site in Australia. ECMWF simulation is in red, LST simulation in blue while black dots represents in-situ measured data.

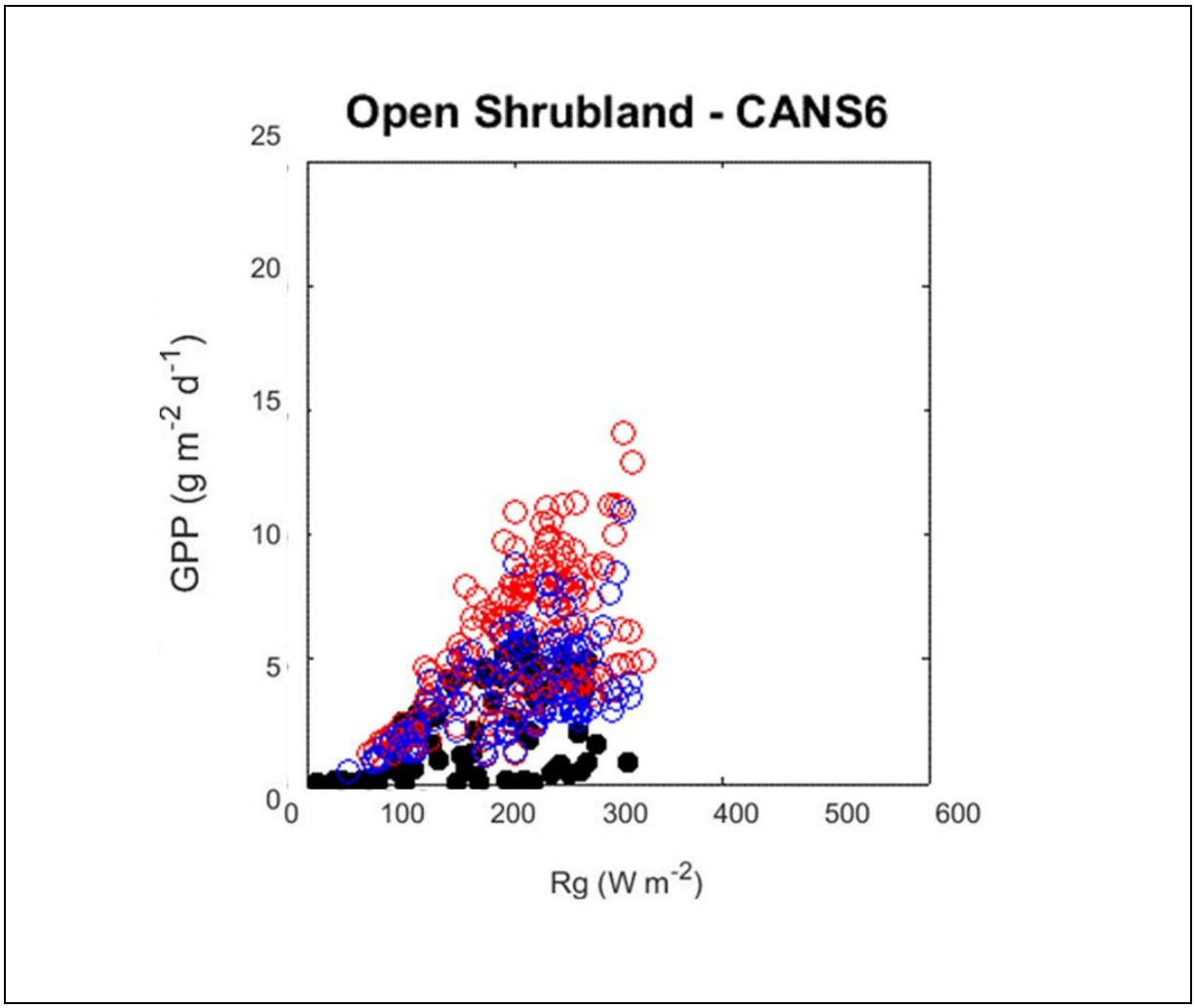

Figure 20: GPP response curves to global radiation (Rg) for an open shrubland site in Canada. ECMWF simulation is in red, LST simulation in blue while black dots represents in-situ measured data.

4.5. COMPARISON OF IN-SITU AND ECMWF CLIMATOLOGICAL FORCING

In order to analyze the mismatch between in-situ and ECMWF forcing variables used as inputs of the model, Figs. 21-28 show the comparison for air temperature (Ta), vapor pressure deficit (VPD) and global radiation (Rg) for eight different sites. It is clear that ECMWF forcings show a good correlation with the in-situ observations. Figs. 29-34 show the comparison for LST and fluxnet Ta for six different sites. LST forcing tends to overestimate in-situ Ta.

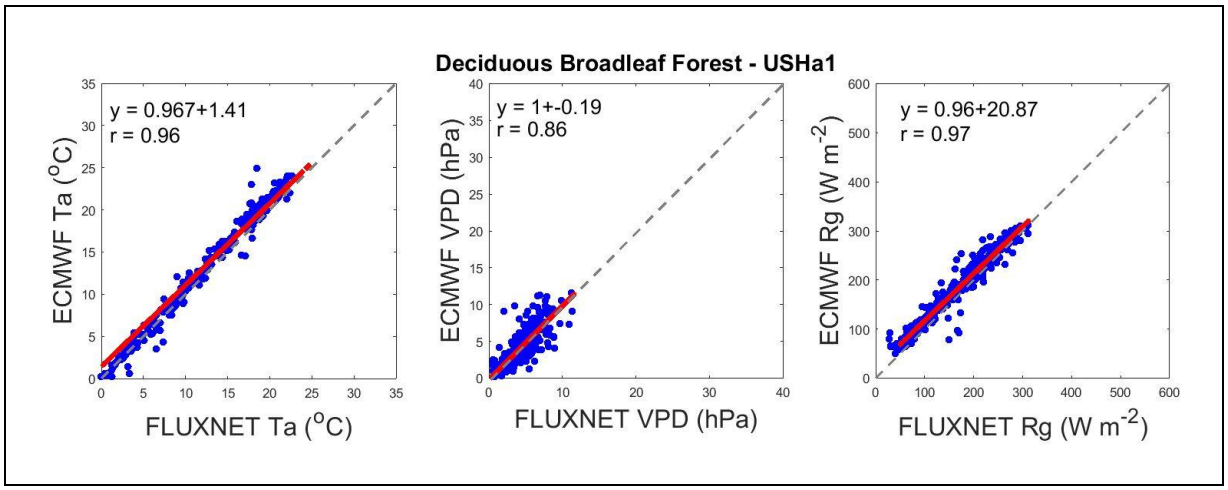

Figure 21: Comparison of in-situ and ERA-I forcing for a deciduous broadleaf forest in US: air temperature (Ta); vapor pressure deficit (VPD); and global radiation (Rg). Red lines represent the linear fit to the data and the grey dotted lines are 1:1 lines. The coefficients of the linear fit and the correlation coefficients are shown in top left corner of the panels.

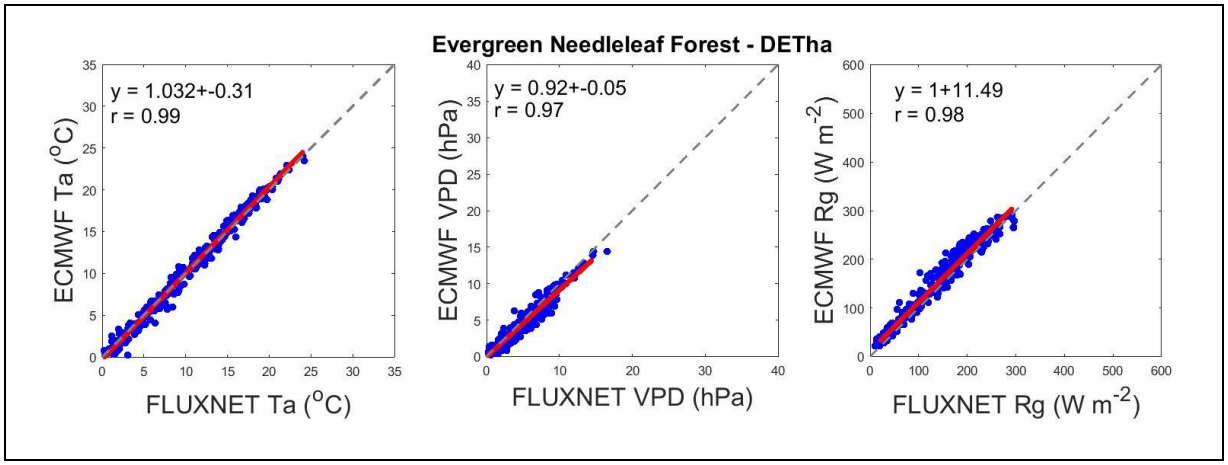

Figure 22: Same as in Fig. 20, expected for an evergreen need leaf forest in Germany.

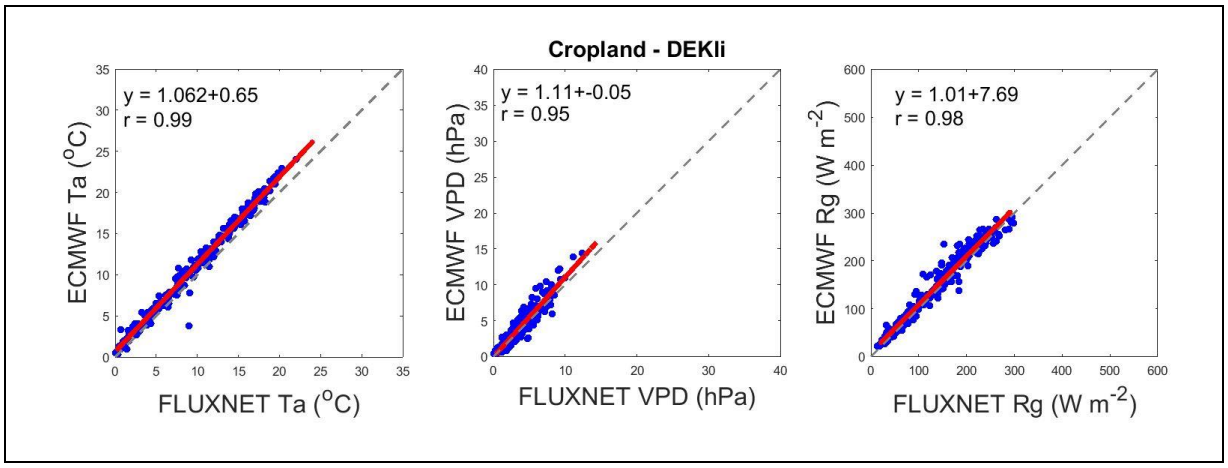

Figure 23: Same as in Fig. 20, expected for a cropland site in Germany.

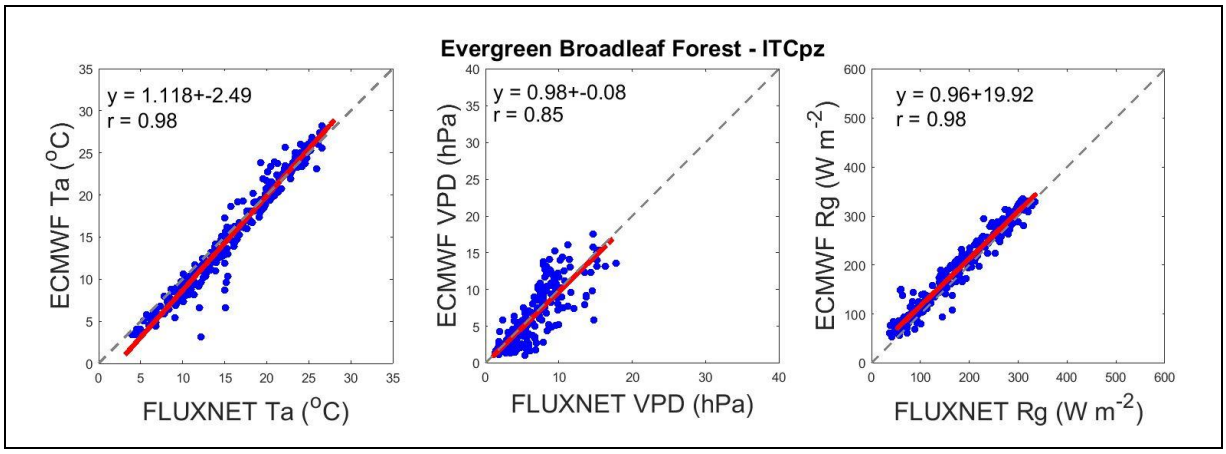

Figure 24: Same as in Fig. 20, expected for an evergreen broadleaf forest in Italy.

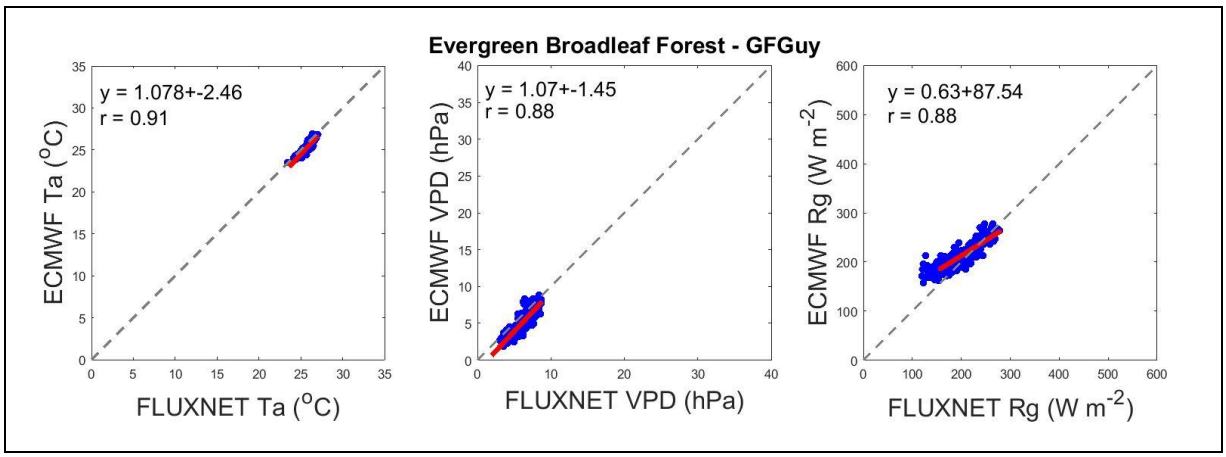

Figure 25: Same as in Fig. 20, expected for an evergreen broadleaf forest in French Guyana.

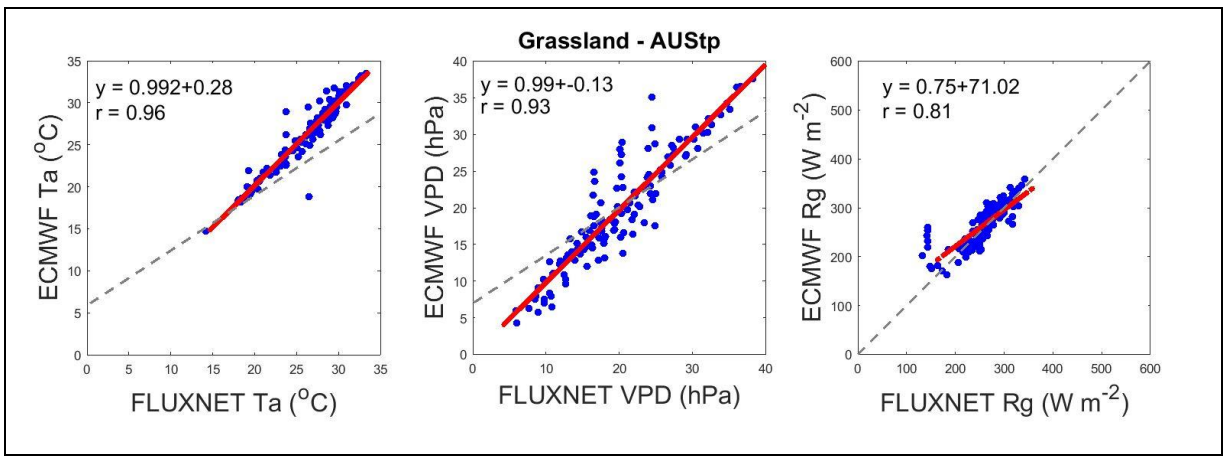

Figure 26: Same as in Fig. 20, expected for an grassland in Australia.

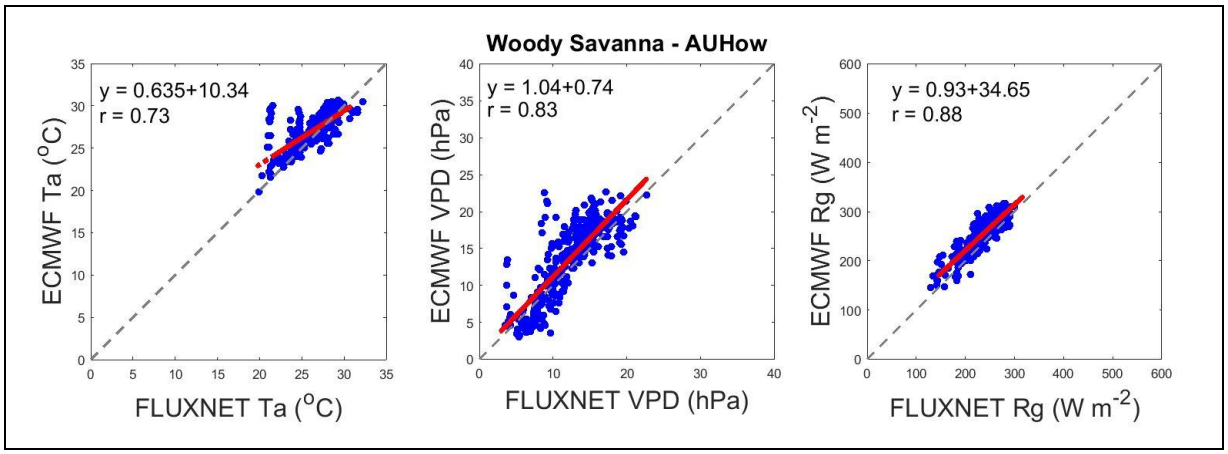

Figure 27: Same as in Fig. 20, expected for an woody savanna in Australia.

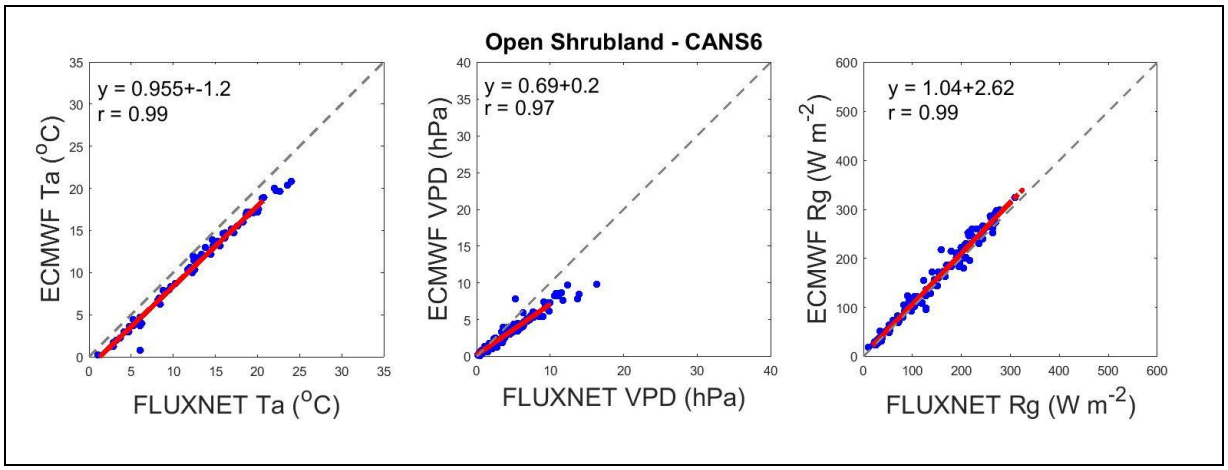

Figure 28: Same as in Fig. 20, expected for an open shrubland in Canada.

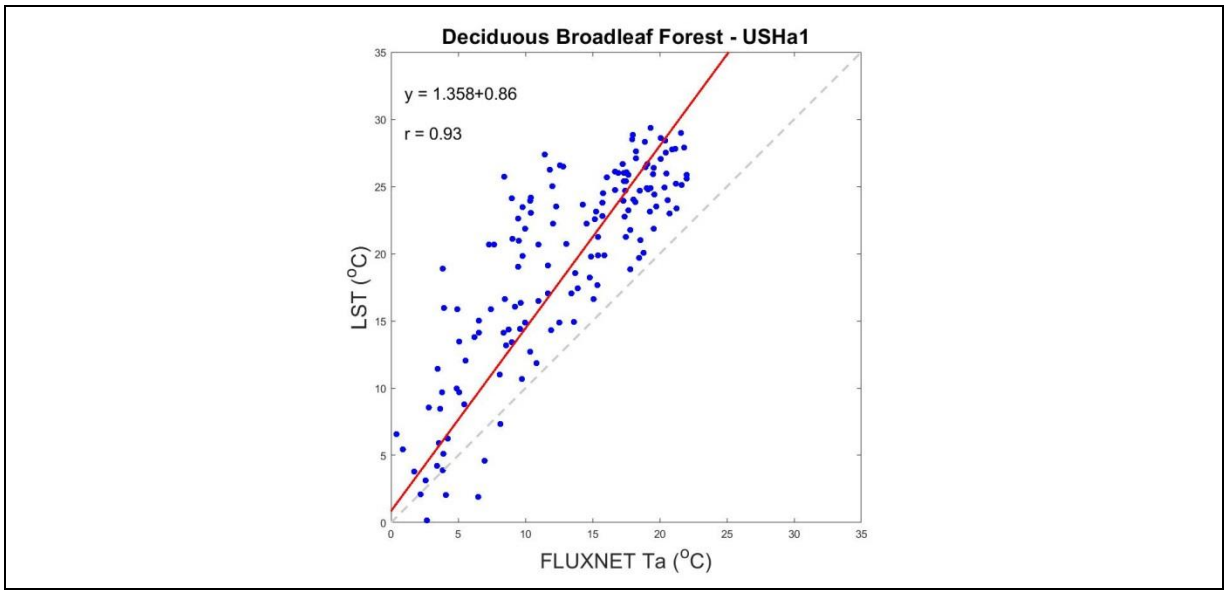

Figure 29: Comparison of in-situ air temperature (Ta) and LST forcing for a deciduous broadleaf forest in US. Red lines represent the linear fit to the data and the grey dotted lines are 1:1 lines. The coefficients of the linear fit and the correlation coefficients are shown in top left corner of the panels.

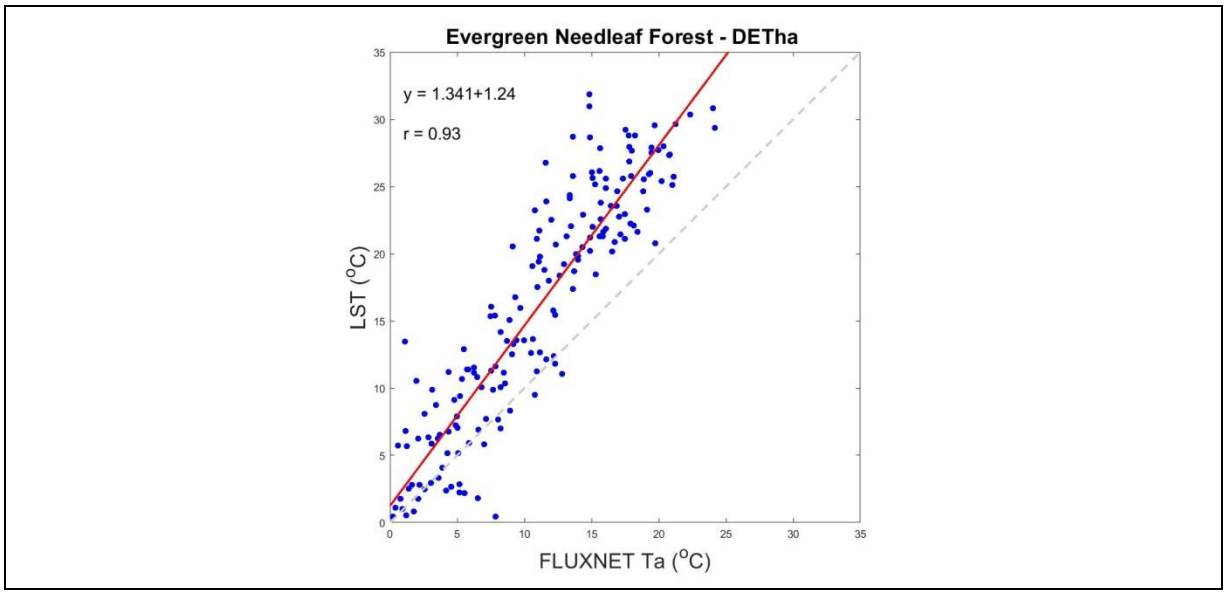

Figure 30: Same as in Fig. 29, expected for an evergreen need leaf forest in Germany.

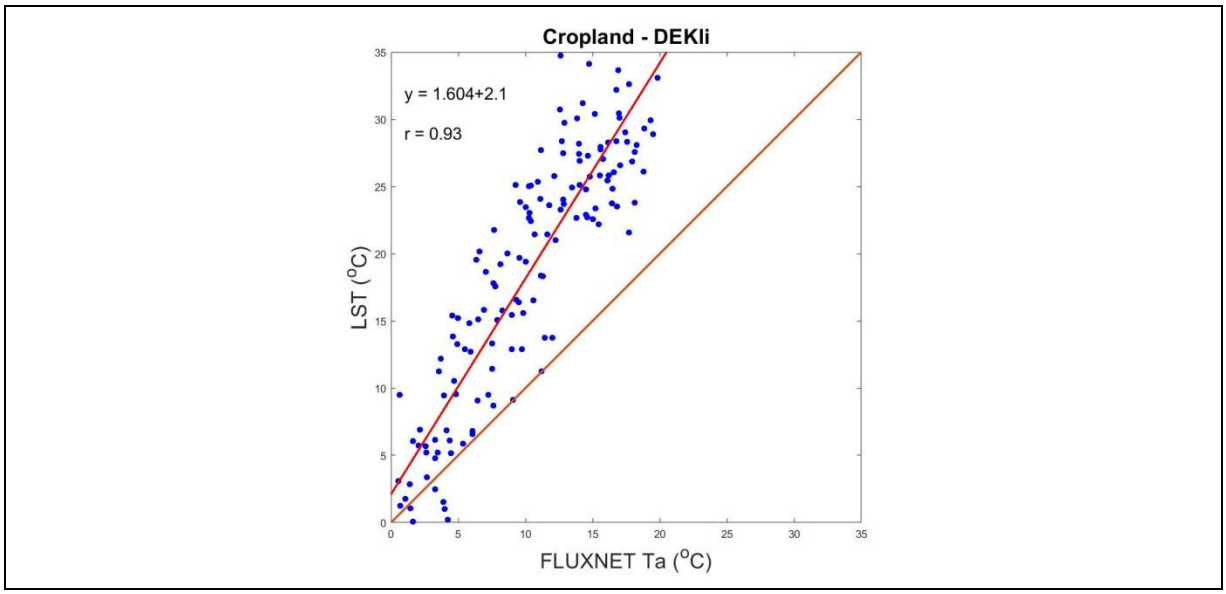

Figure 31: Same as in Fig. 29, expected for a cropland site in Germany.

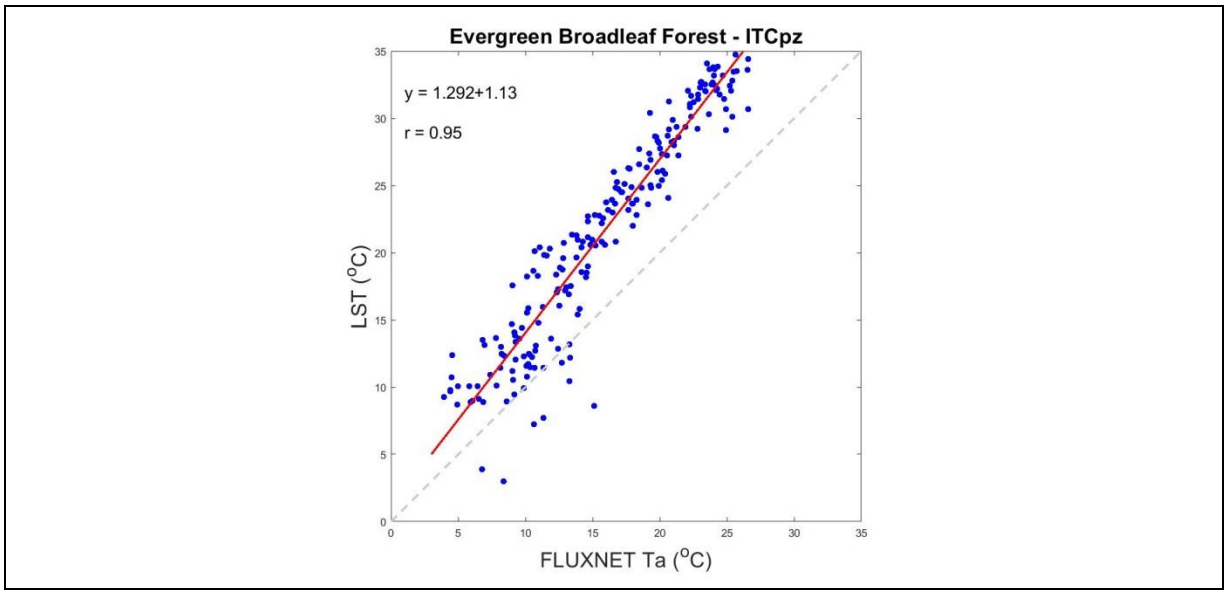

Figure 32: Same as in Fig. 29, expected for an evergreen broadleaf forest in Italy.

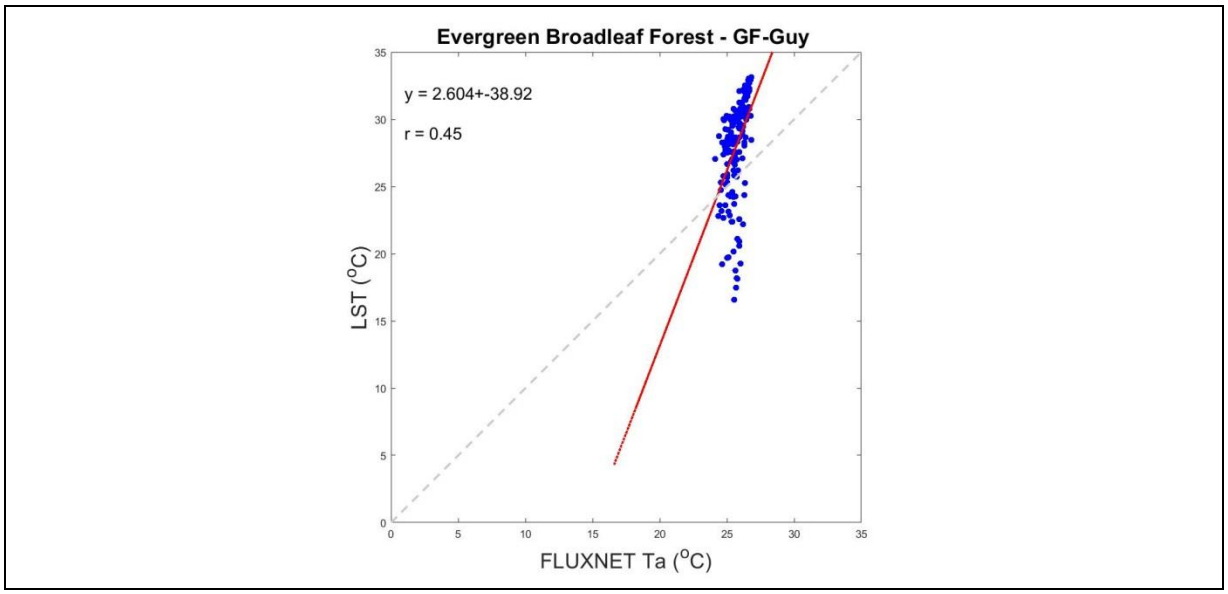

Figure 33: Same as in Fig. 29, expected for an evergreen broadleaf forest in French Guyana.

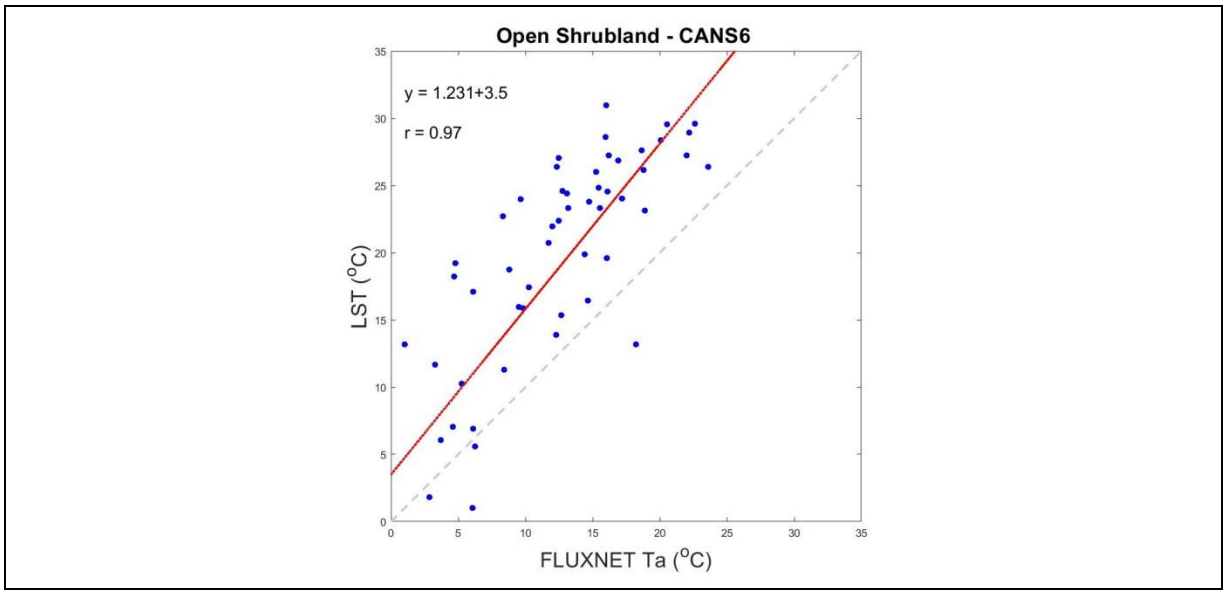

Figure 34: Same as in Fig. 29, expected for an open shrubland in Canada.

CHAPTER 5 CONCLUSIONS

5.1. GENERAL CONCLUSIONS

This report has evaluated the performance of the P model, as implemented in TerrA-P, by comparison with in-situ flux measurements. Two model implementations have been assessed. In one, spatially interpolated ECMWF meteorological data were used to provide dekad temperature values, both for direct input to the model and for the calculation of vpd as an input to the model. In the other, remotely sensed LST data have been used instead of meteorological data.

Comparisons of model and measurements have been made at three levels: (1) at the dekad time scale, with results summarized by performance statistics for each biome; (2) at the annual time scale, focusing on the model's ability to reproduce between-site variations of annual GPP within each ecosystem; (3) at the multi-annual time scale, focusing on the model's ability to reproduce between-year variability, with results summarized within ecosystems.

The most important findings are as follows:

- The model reproduces dekad GPP well in nearly all ecosystems, despite the absence of any biome-specific parameters in the model.
- Exceptions are open shrublands and wetlands. The model systematically overestimates GPP for open shrublands by about 50% and for wetlands by about 100%, regardless of whether LST or ECMWF data are used. For open shrublands, this is most likely because the model does not take into account the impact of soil moisture on LUE (Stocker et al., 2018). For wetlands, the problem may lie either in the impact of inondation on fAPAR retrieval or in an unaccounted-for impact of anoxia on LUE.
- Spatial patterns of annual GPP (represented by between-site differences) are reasonably well simulated. The use of LST reduces the magnitude of biases relative to the use of ECMWF data.
- Interannual variability of GPP is captured to some degree for all ecosystems except for WET and OSH. Also for this analysis the use LST improve the model simulations.
- Mismatches sometimes occur between the modelled and observed seasonal cycles. In the case of broad-leaved evergreen forests in relatively dry regions, GPP overestimates during part of some summers are likely due to the neglect of soil moisture effects. In the case of crops, too-soon modelled greenup may be due to a mismatch between the fAPAR pixel(s) and the actual extent of the crop.
- Comparsions of modelled and empirical response functions for the relationship between GPP and solar radiation confirm that the LST-driven model results are generally consistent with observed relationships.

REFERENCES

Reference

Baldocchi, D.: Breathing of the terrestrial biosphere: lessons learned from a global network of carbon dioxide flux measurement
system, Aust. J. Bot., 56, 1–26, 2008.

Balzarolo, M., Boussetta, S., Balsamo, G., Beljaars, A., Maignan, F., Calvet, J.-C., Lafont, S., Barbu, A., Poulter, B., Chevallier, F., Szczypta, C., and Papale, D.: Evaluating the potential of large-scale simulations to predict carbon fluxes of terrestrial ecosystems over a European Eddy Covariance network, Biogeosciences, 11, 2661–2678, 2014.

Papale, D., Reichstein, M., Aubinet, M., Canfora, E., Bernhofer, C., Kutsch, W., Longdoz, B., Rambal, S., Valentini, R., Vesala, T., and Yakir, D.: Towards a standardized processing of Net Ecosystem Exchange measured with eddy covariance technique: algorithms and uncertainty estimation, Biogeosciences, 3, 571–583, doi:10.5194/bg-3-571-2006, 2006.

Peel, M. C., Finlayson, B. L., and McMahon, T. A.: Updated world map of the Köppen-Geiger climate classification, Hydrol, Earth Syst. Sci., 11, 1633–1644, 2007.

Reichstein, M., Falge, E., Baldocchi, D., Papale, D., Valentini, R., Aubinet, M., Berbigier, P., Bernhofer, C., Buchmann, N., Gilmanov, T., Granier, A., Grünwald, T., Havräankovä, K., Janous, D., Knohl, A., Laurela, T., Lohila, A., Loustau, D., Matteucci, G., Meyers, T., Miglietta, F., Ourcival, J.-M., Rambal, S., Rotenberg, E., Sanz, M., Seufert, G., Vaccari, F., Vesala, T., and Yakir, D.: On the separation of net ecosystem exchange into assimilation and ecosystem respiration: review and improved algorithm, Glob. Change Biol., 11, 1424–1439, 2005.

Stocker, B. D., Zscheischler, J. , Keenan, T. F., Prentice, I. C., Peñuelas, J., and I. Seneviratne, S. Quantifying soil moisture impacts on light use efficiency across biomes. Accepted in New Phytologist, 2018.